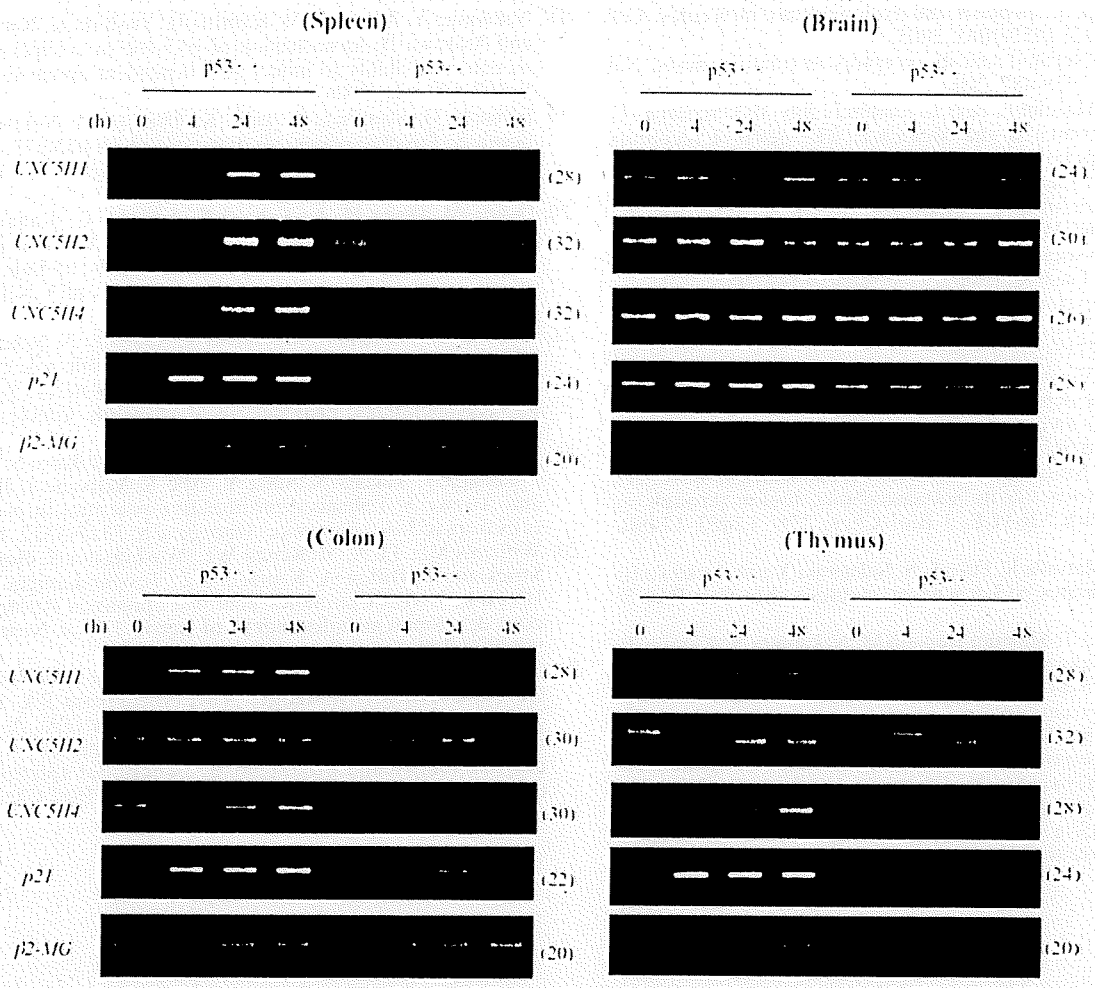

Figure 6. Potential in vivo role of UNC5A in p53-regulated response to DNA damage. RT-PCR results indicated expression levels of UNC5H1, UNC5H2, UNC5H4, and p21 mRNA in the spleen, brain, colon and thymus tissues. Each tissue was isolated from $p53^{+/+}$ and $p53^{-/-}$ mice 24 h after irradiation with γ-ray (10 Gy). The number of cycles for each RT-PCR is indicated in parentheses. β2-MG was used as a loading control.

is probably involved in caspase-dependent apoptosis and that there is most likely a common mechanism for UNC5-induced apoptosis.

All three UNC5s strongly induced apoptosis in the LS174T and SH-SY5Y cells, which contain wild-type p53. However, in the SKNAS and U373MG cells, which contain mutant p53, the ability of the three UNC5s to induce apoptosis differed. For example, UNC5B was able to strongly induce apoptosis whereas UNC5A and UNC5D were not. In particular, UNC5D revealed weaker ability to induce apoptosis in SKNAS and U373MG cells, both of which contain mutant p53. These results are consistent with those reported by Wang et al, where UNC5D was found to amplify the p53-dependent apoptotic response (16). We propose that apoptosis induced by UNC5s may depend on not only the cell type but also the p53 status. The p53 status probably affects UNC5A- or UNC5D-induced apoptosis. Further studies will enable a better understanding of the precise role of UNC5s as dependence receptors and in p53-dependent apoptosis.

Acknowledgements

We thank S. Ikawa for the plasmids of p73α, p73ß, p63α, and p63γ, A. Nakagawara for the plasmid of UNC5D, S. Aizawa for p53-deficient mice. We also thank S. Usuda, and I. Hyo for their technical assistance. This work was supported in part by grants (H.A.) from the Ministry of Health, Labor and Welfare, Japan, and the Ministry of Education, Culture, Sports, Science and Technology, Japan.

References

1. Nakamura Y: Isolation of p53-target genes and their functional analysis. Cancer Sci 95: 7-11, 2004.
2. Kamino H, Futamura M, Nakamura Y, Kitamura N, Kabu K and Arakawa H: B-cell linker protein prevents aneuploidy by inhibiting cytokinesis. Cancer Sci 99: 2444-2454, 2008.
3. Vousden KH and Lu X: Live or let die: the cell's response to p53. Nat Rev Cancer 2: 594-604, 2002.
4. Keino-Masu K, Masu M, Hinck L, Leonardo ED, Chan SS, Culotti JG and Tessier-Lavigne M: Deleted in colorectal cancer (DCC) encodes a netrin receptor. Cell 87: 175-185, 1996.
5. Leonardo ED, Hinck L, Masu M, Keino-Masu K, Ackerman SL and Tessier-Lavigne M: Vertebrate homologues of C. elegans UNC-5 are candidate netrin receptors. Nature 386: 833-838, 1997.
6. Mehlen P, Rabizadeh S, Snipas SJ, Assa-Munt N, Salvesen GS and Bredesen DE: The DCC gene product induces apoptosis by a mechanism requiring receptor proteolysis. Nature 395: 801-804, 1998.
7. Bredesen DE, Mehlen P and Rabizadeh S: Receptors that mediate cellular dependence. Cell Death Differ 12: 1031-1043, 2005.

8. Arakawa H: p53, apoptosis and axon-guidance molecules. Cell Death Differ 12: 1057-1065, 2005.
9. Arakawa H: Netrin-1 and its receptors in tumorigenesis. Nat Rev Cancer 4: 978-987, 2004.
10. Thiebault K, Mazelin L, Pays L, Llambi F, Joly MO, Scoazec JY, Saurin JC, Romeo G and Mehlen P: The netrin-1 receptors UNC5H are putative tumor suppressors controlling cell death commitment. Proc Natl Acad Sci USA 100: 4173-4178, 2003.
11. Bernet A, Mazelin L, Coissieux MM, Gadot N, Ackerman SL, Scoazec JY and Mehlen P: Inactivation of the UNC5C Netrin-1 receptor is associated with tumor progression in colorectal malignancies. Gastroenterology 133: 1840-1848, 2007.
12. Llambi F, Causeret F, Bloch-Gallego E and Mehlen P: Netrin-1 acts as a survival factor via its receptors UNC5H and DCC. EMBO J 20: 2715-2722, 2001.
13. Forcet C, Ye X, Granger L, Corset V, Shin H, Bredesen DE and Mehlen P: The dependence receptor DCC (deleted in colorectal cancer) defines an alternative mechanism for caspase activation. Proc Natl Acad Sci USA 98: 3416-3421, 2001.
14. Williams ME, Strickland P, Watanabe K and Hinck L: UNC5H1 induces apoptosis via its juxtamembrane region through an interaction with NRAGE. J Biol Chem 278: 17483-17490, 2003.
15. Tanikawa C, Matsuda K, Fukuda S, Nakamura Y and Arakawa H: p53RDL1 regulates p53-dependent apoptosis. Nat Cell Biol 5: 216-223, 2003.
16. Wang H, Ozaki T, Shamim Hossain M, Nakamura Y, Kamijo T, Xue X and Nakagawara A: A newly identified dependence receptor UNC5H4 is induced during DNA damage-mediated apoptosis and transcriptional target of tumor suppressor p53. Biochem Biophys Res Commun 370: 594-598, 2008.
17. Masuda Y, Futamura M, Kamino H, Nakamura Y, Kitamura N, Ohnishi S, Miyamoto Y, Ichikawa H, Ohta T, Ohki M, Kiyono T, Egami H, Baba H and Arakawa H: The potential role of DFNA5, a hearing impairment gene, in p53-mediated cellular response to DNA damage. J Hum Genet 51: 652-664, 2006.
18. Nakamura Y, Futamura M, Kamino H, Yoshida K, Nakamura Y and Arakawa H: Identification of p53-46F as a super p53 with an enhanced ability to induce p53-dependent apoptosis. Cancer Sci 97: 633-641, 2006.
19. Ishimoto O, Kawahara C, Enjo K, Obinata M, Nukiwa T and Ikawa S: Possible oncogenic potential of DeltaNp73: a newly identified isoform of human p73. Cancer Res 62: 636-641, 2002.
20. Osada M, Ohba M, Kawahara C, Ishioka C, Kanamaru R, Katoh I, Ikawa Y, Nimura Y, Nakagawara A, Obinata M and Ikawa S: Cloning and functional analysis of human p51, which structurally and functionally resembles p53. Nat Med 4: 839-843, 1998.
21. Futamura M, Kamino H, Miyamoto Y, Kitamura N, Nakamura Y, Ohnishi S, Masuda Y and Arakawa H: Possible role of semaphorin 3F, a candidate tumor suppressor gene at 3p21.3, in p53-regulated tumor angiogenesis suppression. Cancer Res 67: 1451-1460, 2007.
22. Tsukada T, Tomooka Y, Takai S, Ueda Y, Nishikawa S, Yagi T, Tokunaga T, Takeda N, Suda Y, Abe S, Matsuno I, Ikawa Y and Aizawa S: Enhanced proliferative potential in culture of cells from p53-deficient mice. Oncogene 8: 3313-3322, 1993.
23. Williams ME, Lu X, McKenna WL, Washington R, Boyette A, Strickland P, Dillon A, Kaprielian Z, Tessier-Lavigne M and Hinck L: UNC5A promotes neuronal apoptosis during spinal cord development independent of netrin-1. Nat Neurosci 9: 996-998, 2006.
24. Thornberry NA, Rano TA, Peterson EP, Rasper DM, Timkey T, Garcia-Calvo M, Houtzager VM, Nordstrom PA, Roy S, Vaillancourt JP, Chapman KT and Nicholson DW: A combinatorial approach defines specificities of members of the caspase family and granzyme B. Functional relationships established for key mediators of apoptosis. J Biol Chem 272: 17907-17911, 1997.

Oncogene (2009) 28, 3081–3092

www.nature.com/onc

ORIGINAL ARTICLE

XEDAR as a putative colorectal tumor suppressor that mediates p53-regulated anoikis pathway

C Tanikawa[1,3], Y Furukawa[2], N Yoshida[3], H Arakawa[4], Y Nakamura[1] and K Matsuda[1]

[1]*Laboratory of Molecular Medicine, Human Genome Center, The University of Tokyo, Tokyo, Japan;* [2]*Division of Clinical Genome Research, The University of Tokyo, Tokyo, Japan;* [3]*Division of Gene Expression and Regulation, Institute of Medical Science, The University of Tokyo, Tokyo, Japan and* [4]*Cancer Medicine and Biophysics Division, National Cancer Center Research Institute, Tokyo, Japan*

Colorectal cancers with mutations in the *p53* gene have an invasive property, but its underlying mechanism is not fully understood. Through the screening of two data sets of the genome-wide expression profile, one for p53-introduced cells and the other for the numbers of cancer tissues, we report here X-linked ectodermal dysplasia receptor (XEDAR), a member of the TNFR superfamily, as a novel p53 target that has a crucial role in colorectal carcinogenesis. p53 upregulated XEDAR expression through two p53-binding sites within intron 1 of the XEDAR gene. We also found a significant correlation between decreased *XEDAR* expressions and *p53* gene mutations in breast and lung cancer cell lines ($P=0.0043$ and $P=0.0122$, respectively). Furthermore, promoter hypermethylation of the *XEDAR* gene was detected in 20 of 20 colorectal cancer cell lines (100%) and in 6 of 12 colorectal cancer tissues (50%), respectively. Thus, the *XEDAR* expression was suppressed to <25% of surrounding normal tissues in 12 of 18 colorectal cancer tissues (66.7%) due to either its epigenetic alterations and/or *p53* mutations. We also found that XEDAR interacted with and subsequently caused the accumulation of FAS protein, another member of p53-inducible TNFR. Moreover, XEDAR negatively regulated FAK, a central component of focal adhesion. As a result, inactivation of XEDAR resulted in the enhancement of cell adhesion and spreading, as well as resistance to p53-induced apoptosis. Taken together, our findings showed that XEDAR is a putative tumor suppressor that could prevent malignant transformation and tumor progression by regulating apoptosis and anoikis.

Oncogene (2009) **28,** 3081–3092; doi:10.1038/onc.2009.154; published online 22 June 2009

Keywords: XEDAR; P53; FAS; colorectal cancer; anoikis; TNFR

Correspondence: Assistant Professor K Matsuda, Laboratory of Molecular Medicine, Human Genome Center, Institute of Medical Science, The University of Tokyo, 4-6-1 Shirokanedai, Minato, Tokyo 108-8639, Japan.
E-mail: koichima@ims.u-tokyo.ac.jp
Received 21 October 2008; revised 11 March 2009; accepted 12 May 2009; published online 22 June 2009

Introduction

Identification and characterization of cancer-related genes are critical steps for the understanding of carcinogenic mechanisms. Among the cancer-related genes that have been identified so far, inactivation of the *p53* gene is the most common alteration observed in human cancers (Beroud and Soussi, 2003; Hollstein *et al.*, 1994). In response to various types of cellular stress, including DNA damage, aberrant growth signal and oxidative stress, the p53 protein is stabilized and accumulated. Activated p53 regulates many target genes that induce cell-cycle arrest, apoptosis, DNA repair and cellular senescence (Levine, 1997; Vogelstein *et al.*, 2000). We have isolated a number of p53 target genes, including p53AIP1, p53R2 and p53RDL1 (Nakamura, 2004; Oda *et al.*, 2000; Tanaka *et al.*, 2000; Tanikawa *et al.*, 2003), and implicated the molecular mechanisms by which p53 regulated cell fate, death or survival, by balancing the expression levels of these genes. However, an entire picture of the p53 signaling pathway has not been disclosed yet.

In this study, to identify a p53 target gene(s) that is indispensable for p53-dependent tumor suppression, we used two data sets of the genome-wide expression profile obtained by cDNA microarray consisting of 36 864 cDNA fragments. One data set was obtained using the cells in which wild-type p53 was exogenously introduced, and the other was obtained using more than 1000 clinical cancer cases (Kidokoro *et al.*, 2008; Kitahara *et al.*, 2001). Through the analysis of these two data sets, we identified XEDAR (X-linked ectodermal dysplasia receptor, also known as EDA2R and TNFRSF27) as a novel p53 target, which mediated important p53 functions.

The X-linked ectodermal dysplasia receptor is a member of the TNFR superfamily that is divided into two subgroups because of difference in their cytoplasmic region. One class of TNFR, a death receptor, contains a cytoplasmic death domain. Several death receptors, such as FAS, and four TRAIL receptors, DR4, DR5, DcR1 and DcR2, were shown to be regulated by p53 (Liu *et al.*, 2005; Wu *et al.*, 1997) and their physiological roles in carcinogenesis have been well characterized (Lee *et al.*, 1999; Takakuwa *et al.*, 2002). XEDAR belongs to the other class of TNFR that lacks a discernible death domain. This class of TNFRs interacts with TRAFs (TNFR-associated factors) and activates the nuclear

factor-κB (NF-κB) signaling, and consequently promotes cell proliferation. On the other hand, some members of this subclass were indicated to be involved in apoptotic pathways (Afford *et al*., 1999). Thus, the TNFR superfamily is involved in various signaling pathways, including immune response, inflammation, development and carcinogenesis.

EDA-A1 and EDA-A2 are two major splicing isoforms of EDA, and EDA-A2 specifically binds to XEDAR (Yan *et al*., 2000). EDA-A1 binds to EDAR and has an essential role for proper formation of skin appendages, as the mutations of *EDA*, *EDAR* or its adaptor protein *EDARADD* were shown to cause hypohidrotic ectodermal dysplasia (Smahi *et al*., 2002). XEDAR is highly expressed in epidermal tissues during embryogenesis (Yan *et al*., 2000), and mice that lacked TRAF6, an adaptor protein of XEDAR, also displayed hypohidrotic ectodermal dysplasia (Naito *et al*., 2002). However, any mutations in the *XEDAR* gene have not been reported in individuals with hypohidrotic ectodermal dysplasia, and *XEDAR*-deficient mice were indistinguishable from their wild-type littermates at birth (Newton *et al*., 2004). Thus, the physiological function of XEDAR has not been well clarified so far.

In this study, we report that XEDAR is frequently inactivated in human colorectal cancers, and its inactivation caused resistance to p53-induced apoptosis and enhancement of cell adhesion. Thus, our findings suggested the crucial role of XEDAR in the anoikis pathway. In a multistep genetic model for colorectal cancer, *p53* mutations are more commonly found in invasive colon cancer tissues (Vogelstein *et al*., 1989), but the mechanisms by which p53 inhibits metastasis have not been fully elucidated (Ilic *et al*., 1998; Nikiforov *et al*., 1996). We show the novel mechanism that p53 suppresses colorectal carcinogenesis and tumor progression by regulating a novel p53 target, XEDAR.

Results

Identification of XEDAR as a p53 target gene

To fully uncover p53 target genes, we examined a total of 36 864 cDNA fragments by means of cDNA microarray using mRNAs isolated from U373MG *p53* mutant glioblastoma cells that were infected with adenovirus designed to express wild-type p53 (Ad-p53) or LacZ (Ad-LacZ) (Tanikawa *et al*., 2003). Thus, we found a total of 60 novel p53 target genes that were upregulated by the exogenous introduction of wild-type p53. We then examined the expression profile database constructed by the same set of cDNA microarray using various cancers (Kitahara *et al*., 2001) and selected XEDAR for further biological analysis because of its frequent downregulation in colorectal cancer tissues. To validate its regulation by p53, we carried out quantitative real-time PCR analysis and northern blot analysis and found that the *XEDAR* expression was remarkably induced by the introduction of p53 but not by that of LacZ (Figure 1a). Moreover, XEDAR protein was increased by Ad-p53 infection in a dose-dependent manner (Supplementary Figure 1). We also investigated the induction of XEDAR by DNA damage using MCF7 (breast cancer) and A549 (lung cancer) cells with wild-type p53. We found that Adriamycin treatment remarkably induced the XEDAR expression in both cells, indicating the p53-dependent regulation of XEDAR expression (Figure 1b).

Subsequently, we surveyed the genomic sequence of the *XEDAR* gene that is located on chromosome Xq12 and found two putative p53-binding regions (p53BR1 and p53BR2) within the first intron (Figure 1c). To examine the possible binding of p53 to these DNA segments, we carried out a chromatin immunoprecipitation (ChIP) assay using U373MG cells that were infected with either Ad-p53 or Ad-LacZ. A PCR analysis of immunoprecipitated DNA indicated that the p53 protein bound to the genomic fragment, including p53BR1 (Figure 1c). We then subcloned a DNA fragment of 466 base pairs corresponding to p53BR1, which included four putative p53-binding sequences (BS-A to D, respectively, Figure 1d) into the pGL3 promoter vector (pGL3/p53BR1) (Promega, Madison, WI, USA). We found that the co-transfection of pGL3/p53BR1 with wild-type p53 expression plasmid enhanced the luciferase activity more than 40-fold, whereas the base substitutions within BS-A and BS-B segments completely diminished the luciferase activity (Figures 1c and d). The result of ChIP analysis suggested the weak association of p53 with p53BR2, but co-

Figure 1 Identification of *XEDAR* as a novel p53 target gene. (**a**) Shows the quantitative PCR (qPCR) analysis (upper) and northern blot analysis (lower) of X-linked ectodermal dysplasia receptor (*XEDAR*) transcript in U373MG cells at indicated times after infection with Ad-p53 or Ad-LacZ at 8 multiplicity of infection (MOI). *β2-Microglobulin* and *β-actin* were used for the normalization of expression levels. $p21^{WAF1}$ was served as a positive control. (**b**) Shows the qPCR analysis (upper) and western blot analysis (lower) of XEDAR at 48 h after treatment with adriamycin (ADR) in MCF7 and A549 cells. *β2-Microblobulin* and β-actin were used for the normalization of expression levels. (**c**) Represents the genomic structure of the *XEDAR* gene (upper). Black boxes indicate the locations and relative sizes of seven exons. The arrows indicate the potential p53-binding regions (p53BR1 and p53BR2). Chromatin immunoprecipitation (ChIP) assay was carried out using U373MG cells that were infected with Ad-p53 (lanes 1, 3–5) or Ad-LacZ (lane 2) (middle). DNA–protein complexes were immunoprecipitated with an anti-p53 antibody (lanes 2 and 3) followed by PCR amplification. Input chromatin represents a portion of the sonicated chromatin before immunoprecipitation (lane 1). Immunoprecipitates with an anti-Flag antibody (lane 4) or in the absence of antibody (lane 5) were used as negative controls. Results of luciferase assay of p53BR1 and p53BR2 are shown (lower). Luciferase activity is indicated relative to the activity of mock vector. (**d**) Shows the genomic structure of p53BR1 (upper). The arrows indicate the locations of p53BSs (BS-A to D) in p53BR1. Comparison of each p53BS with the consensus sequence (middle). R, purine; W, A or T; Y, pyrimidine. Identical nucleotides to the consensus sequence are written in capital letters. The underlined cytosine and guanine were substituted for thymine to introduce mutation at each p53-binding site. Results of luciferase assay of p53BR1 with or without mutations at either of p53BS are shown (lower). Luciferase activity is indicated relative to the activity of mock vector.

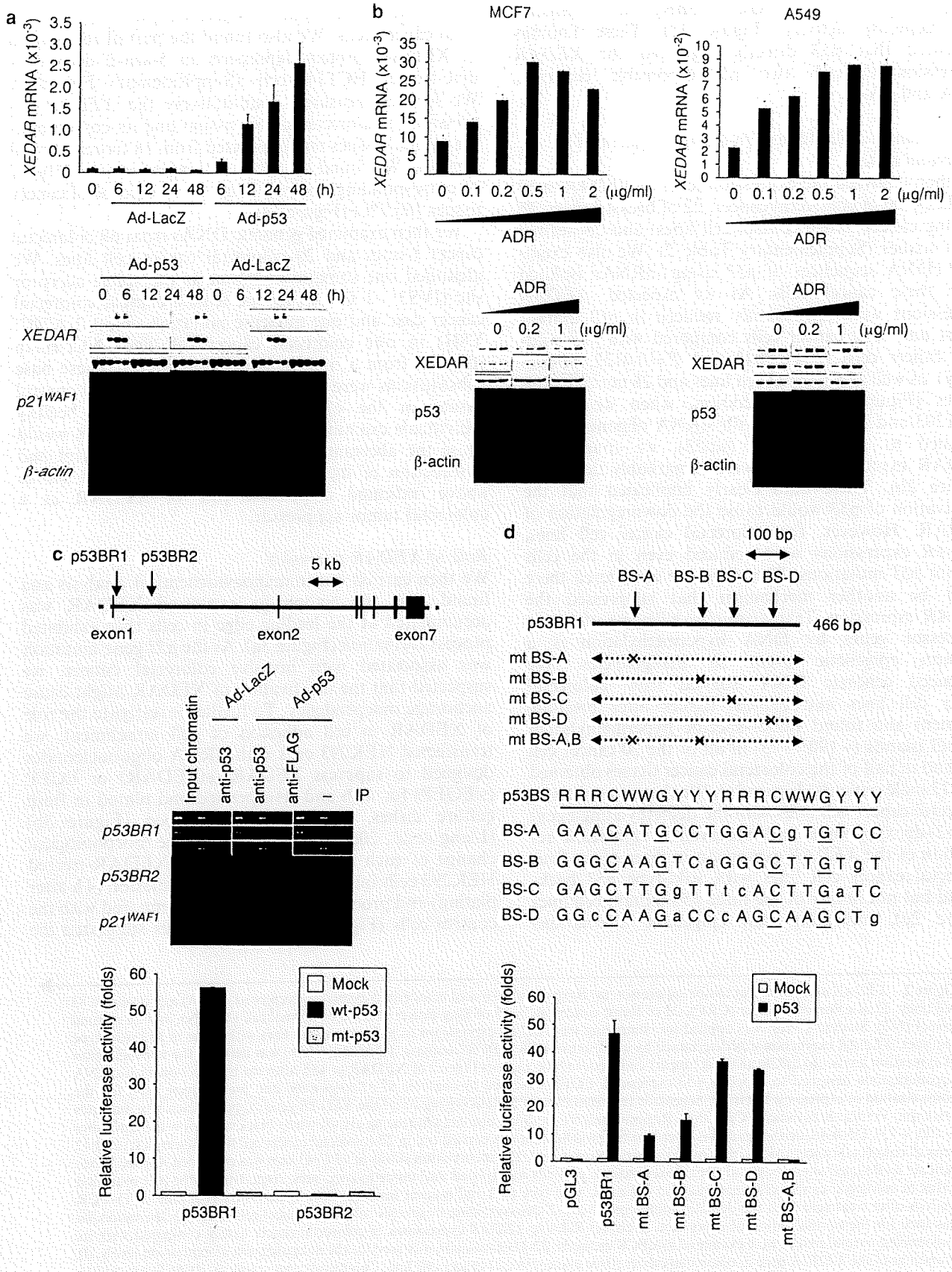
a
XEDAR mRNA (x10-3)
3.5
3.0
2.5
2.0
1.5
1.0
0.5
0
0 6 12 24 48 6 12 24 48 (h)
Ad-LacZ
Ad-p53
b
MCF7
A549
XEDAR mRNA (x10-3)
XEDAR mRNA (x10-2)
0 0.1 0.2 0.5 1 2 (μg/ml)
ADR
Ad-p53
Ad-LacZ
0 6 12 24 48 0 6 12 24 48 (h)
XEDAR
p21WAF1
β-actin
0 0.2 1 (μg/ml)
p53
c
p53BR1
p53BR2
5 kb
exon1
exon2
exon7
Input chromatin
anti-p53
anti-p53
anti-FLAG
IP
p53BR1
p53BR2
p21WAF1
Relative luciferase activity (folds)
Mock
wt-p53
mt-p53
d
100 bp
BS-A
BS-B
BS-C
BS-D
466 bp
mt BS-A
mt BS-B
mt BS-C
mt BS-D
mt BS-A,B
p53BS R R R C W W G Y Y Y R R R C W W G Y Y Y
BS-A G A A C A T G C C T G G A C g T G T C C
BS-B G G G C A A G T C a G G G C T T G T g T
BS-C G A G C T T G g T T t c A C T T G a T C
BS-D G G c C A A G a C C c A G C A A G C T g
Mock
p53
pGL3
p53BR1
mt BS-A
mt BS-B
mt BS-C
mt BS-D
mt BS-A,B

transfection of p53 with pGL3/p53BR2 did not enhance the luciferase activity (Figure 1c). These findings indicated that p53 directly regulated the *XEDAR* expression through two p53-responsible elements, BS-A and BS-B.

Expression of XEDAR was frequently suppressed in colorectal cancer

We then analyzed the expression level of *XEDAR* in 83 cell lines (20 of colorectal cancer, 22 of breast cancer, 35 of lung cancer and 6 control cell lines) and 26 normal adult tissues (Supplementary Table 2). We also examined cDNA sequences of *p53* using mRNAs isolated from these cancer cells. As we expected, *XEDAR* expressions were significantly reduced in *p53* mutant breast and lung cancer cells compared with *p53* wild-type cancer cells ($P=0.0043$ and $P=0.0122$, respectively), as well as 6 normal cell lines and 26 normal adult tissues (Figure 2a). In addition, when we treated HEK293 and NHDF cells with siRNA oligonucleotide designed to suppress p53 (sip53), we found that XEDAR expression levels were remarkably decreased (Figure 2b). These data clearly implicated that the inactivation of p53 would cause the downregulation of XEDAR. However, for colorectal cancer cell lines, *XEDAR* expressions were reduced even in the cells without *p53* mutations. Therefore, we considered there might be another mechanism that suppressed the *XEDAR* expression. Transcriptional silencing of tumor suppressor genes by DNA hypermethylation is a common epigenetic event in malignancies. We sequenced genomic DNA isolated from colorectal cancer cell lines and clinical tissues after bisulfate treatment and found tumor-specific hypermethylation of CpG islands (−190/+73) in all of the 20 cancer cell lines and in half of the colorectal cancer tissues obtained from 12 male patients (Figure 2c). We then treated seven colorectal cancer cell lines with the demethylating agent 5-aza-2′-deoxycytidine and observed a significant restoration of the *XEDAR* expression in three of the four colorectal cancer cell lines with wild-type *p53* background but not in any of the three *p53* mutant cell lines (Figure 2d), indicating that epigenetic alternations contribute to the reduced *XEDAR* expression in colorectal cancer cells. We also found the partial restoration of XEDAR protein expression in 5-aza-2′-deoxycytidine-treated HCT116 cells (Supplementary Figure 2). We further measured quantitatively the *XEDAR* expression in colorectal cancer tissues and its corresponding normal tissues microdissected from 18 frozen clinical samples. We found its decreased expression (<25% of its corresponding normal tissue) in 12 colorectal cancer tissues (66.7%) (Figure 2e).

We then examined genomic DNAs from 68 colorectal cancer tissues and 20 colorectal cancer cell lines. We identified one somatic mutation at the splice acceptor site (IVS3 −1 G>A) in one female clinical colorectal cancer case and one missense mutation (exon 2 A74C; Y8H) in one colorectal cancer cell line, NCI-H716 (derived from a male patient) (Figure 2f). These base substitutions were found in none of the normal control tissues in the 68 patients or 96 normal healthy individuals examined. The splicing site mutation would cause the aberrant splicing of *XEDAR* transcript and dysfunction of the XEDAR protein. The data shown above indicated a possible role of XEDAR as a colorectal tumor suppressor.

Role of XEDAR in anoikis

We then carried out immunocytochemical analysis and found that the ectopically expressed XEDAR was accumulated at the leading edge in cells that exhibited process formation (Figure 3a). As the *p53* gene mutation was associated with invasive colorectal cancer, we suspected that the inactivation of XEDAR might cause anchorage independency. To further investigate the role of XEDAR in cell adhesion or cell attachment, we transfected HEK293 cells with siRNA oligonucleotides designed to suppress XEDAR (siXEDAR) or EGFP (siEGFP) for 48 h and resuspended and plated in fresh culture dishes, as previously described (Figure 3b) (Liang *et al*., 2007). We investigated the morphological change of each cell and found that siXEDAR-treated HEK293 cells indicated increased cell adhesion (4 h after plating) and process formation (12 h) compared with the control cells (Figure 3b). These findings suggested the

Figure 2 *XEDAR* as a colorectal tumor suppressor. (**a**) Boxplots of X-linked ectodermal dysplasia receptor (*XEDAR*) expression in 83 cell lines; 20 of colorectal cancer (CRC), 22 of breast cancer (BC), 35 of lung cancer (LC), 6 of normal cell lines (N), and 26 normal tissues (NT). Student's *t*-test was applied for comparing the *XEDAR* expressions in *p53* mutant cell lines with those in *p53* wild-type cell lines. *XEDAR* expression was determined by quantitative PCR (qPCR) analysis. *β2-Microglobulin* was used for the normalization of expression levels. (**b**) qPCR analysis (upper) and western blot analysis (lower) of XEDAR at 48 h after the transfection with siRNA oligonucleotide designed to suppress p53 expression. EGFP was used as control. *β2-Microglobulin* and β-actin were used for the normalization of expression levels. (**c**) Schematic representation of 5′-flanking region of the *XEDAR* gene (upper). Black box indicates first exon. Vertical bars indicate CpG sites. Regions analyzed by direct bisulfite sequencing are shown by black bar below the CpG sites (−190/+73). DNA sequencing analysis after bisulfite modification was carried out in 20 colorectal cancer cell lines (lower, left) and 12 pairs of colorectal cancer tissues from male patients (lower, right). The methylation status of 13 CpG sites was examined. Closed boxes indicate methylated sites, gray and open boxes indicate partially methylated and unmethylated sites, respectively. The p53 mutation status of colorectal cancer cell lines was also indicated; wild type (wt) and mutant (mt). (**d**) Semi-quantitative real time (RT)–PCR analysis after treatment with the demethylating agent 5-aza-2′-deoxycytidine in several colorectal cancer cell lines. *β2-Microglobulin* was used for the normalization of expression levels. (**e**) Relative *XEDAR* expressions in colorectal cancer tissues compared with its surrounding normal tissues were examined by qPCR methods. *β2-Microglobulin* was used for the normalization of expression levels. (**f**) Mutations of the *XEDAR* gene in colorectal cancer tissue and colorectal cancer cell line. Colorectal cancer tissue (CRC66T) has a G to A substitution at the splice acceptor site. NCI-H716 has a T to C substitution in exon 2 (Tyr8His). Sequences of the corresponding normal tissue (CRC66N) and the control DNA are also shown. Genomic structure and domain structure of XEDAR are shown at the lower panel. The asterisks indicate the location of mutations.

inhibitory effects of XEDAR on cell adhesion and/or motility. The presence of the p53 mutation was indicated to be significantly correlated with metastasis and poor prognosis of various cancers (Diez *et al*., 2000; Pharoah *et al*., 1999). Interestingly, NCI-H716 colon cancer cells carrying mutation in the *XEDAR* gene were non-adherent cells that acquired anchorage independency, whereas the remaining 19 colorectal cancer cells with wild-type *XEDAR* were adherent cells. Hence, we suspected that loss of functional XEDAR might have a

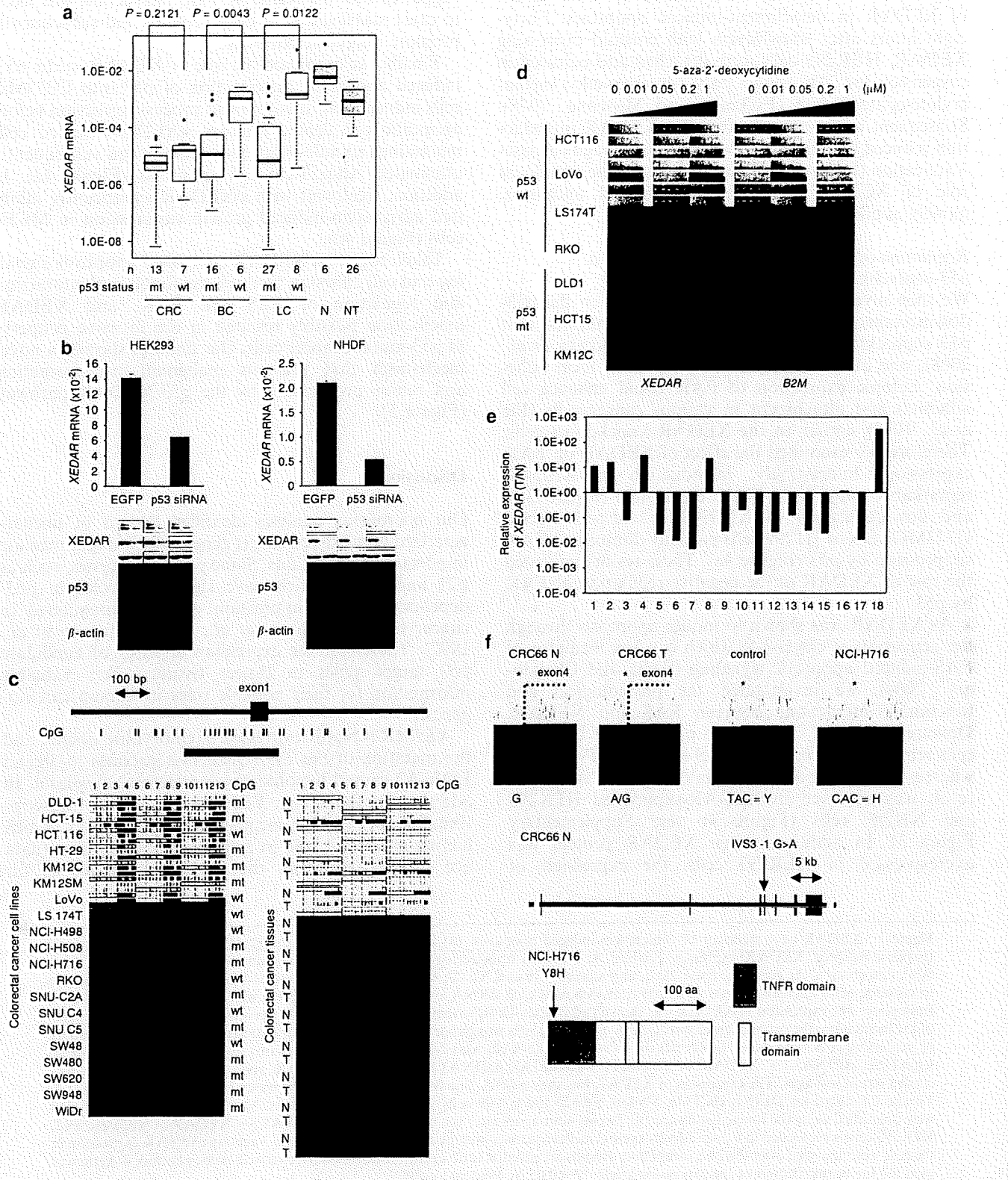

key role in the metastatic property of p53-mutated cancer. We then carried out a colony formation assay in soft agar using cancer cell lines with low or absent expression of *XEDAR* (DLD-1, HCT116, SW480, SW620 and H1299 cells) and found that XEDAR could suppress anchorage-independent tumor cell growth (Figure 3c). Thereafter, we examined the involvement of XEDAR in detachment-induced apoptosis. Forty-eight hours after transfection with plasmid expressing XEDAR, HEK293 cells were detached and cultured in suspension for 24 h using a poly-2-hydroxyethyl methacrylate-coated plate (Folkman and Moscona, 1978). Subsequent analyses indicated that XEDAR introduction reduced the number of viable cells through caspase-3 activation (Figure 3d). Thus, we showed the significant role of XEDAR in detachment-induced apoptosis, namely anoikis.

Regulation of FAS and FAK by XEDAR in a p53-dependent apoptotic pathway

We then investigated the role of XEDAR in the p53-downstream pathway. A recent analysis indicated that p53 suppressed FAK expression (Golubovskaya *et al.*, 2008), one of the essential components in focal adhesion. Ectopic expression of FAK could enhance cell adhesion and attachment in various cancer cells (Ilic *et al.*, 1995) similar to the XEDAR knockdown cells. Therefore, we examined the effect of XEDAR on FAK expression. Interestingly, introduction of XEDAR remarkably suppressed FAK expression (Figure 3d), and downregulation of XEDAR in Ad-p53-infected U373MG cells or H1299 cells partially diminished FAK suppression by p53 (Figure 4a). These results indicated the role of XEDAR in the negative regulation of FAK by p53.

As XEDAR was shown to induce apoptosis through the activation of caspase-8, which is a key mediator of FAS-induced apoptotic signaling (Sinha and Chaudhary, 2004), we investigated the physiological and functional interactions between FAS and XEDAR. Downregulation of XEDAR in p53-infected U373MG cells remarkably suppressed FAS induction (Figure 4a), whereas p21 expression was not affected. A similar result was observed in XEDAR-suppressed HEK293 and NHDF cells (Figure 4b and Supplementary Figure 3). In addition, when XEDAR protein was overexpressed in HEK293 cells, the expression of endogenous FAS protein was significantly increased (Figure 4b). Furthermore, knockdown of FAS also suppressed the expression of XEDAR (Figure 4b). Co-immunoprecipitation or immunocytochemical analysis showed a physiological interaction of XEDAR and FAS at the plasma membrane (Figure 4c). These results suggested that the XEDAR–FAS interaction was likely to cause stabilization of both proteins and subsequently promote apoptotic pathway.

Finally, we examined the role of XEDAR in the p53-induced apoptosis. Introduction of p53 into U373MG cells induced cell rounding and process retraction before apoptotic cell death, whereas siXEDAR-treated cells maintained spindle-shape morphology and subsequently attenuated Ad-p53-induced apoptosis (Figure 4d). In addition, treatment with siXEDAR significantly inhibited adriamycin-induced growth suppression in MCF7 cells (Figure 4d).

Taken together, XEDAR controlled apoptosis signaling and cell adhesion through the functional interaction and regulation of FAS and FAK, and XEDAR inactivation possibly resulted in the invasive property of p53-mutant cancer cells. Our findings showed a novel mechanism that prevents malignant transformation and tumor progression by the p53/XEDAR pathway (Figure 5).

Discussion

Our microarray analysis identified dozens of uncharacterized possible p53 target genes, which might mediate important p53 functions. Some p53 target genes, such as p21 and BAX, which have significant roles in p53-dependent tumor suppression were downregulated in cancer tissues (Furutani *et al.*, 1997; Rampino *et al.*, 1997). Therefore, the expression analysis of candidate p53 target genes in cancer tissues offers valuable information for their possible roles in human carcinogenesis.

XEDAR is highly expressed in embryonic tissues, and the mutation of the *EDA* gene that encodes its ligand EDA-A2 caused hypohidrotic ectodermal dysplasia. In addition, we found that *XEDAR* was a direct transcriptional target of p63, a member of the p53 family, which has an important role in epidermal development (data not shown). However, the evidence obtained so far

Figure 3 XEDAR as a mediator of detachment-induced apoptosis. (**a**) HEK293 cells were transfected with X-linked ectodermal dysplasia receptor (XEDAR) expression plasmid. At 24 h after transfection, the cells were detached and seeded on a fresh plate. After 60 h of incubation, the cells were fixed and double stained with anti-XEDAR antibody (Alexa fluor 488) and Alexa fluor 594 phalloidin to visualize actin filaments. (**b**) At 48 h after transfection of each siRNA into HEK293 cells, the cells were detached and seeded on a fresh plate. The expression of XEDAR was shown (left). After 4 h (spreading assay, middle) or 12 h (processing morphogenesis, right) of the incubation, the proportion of spreading or processing cells was indicated (upper panels). The representative images of spreading or processing cells were shown (lower panels, arrowheads). (**c**) Cells were transfected with either of two plasmids expressing the sense strand (SE, pcDNA3.1+/XEDAR) or the antisense strand (AS, pcDNA3.1-/XEDAR) of XEDAR, and colony formation assay was carried out in soft agar. The expression of XEDAR was shown (left). The cells were cultured in the presence of geneticin (0.4, 0.5, 1.0, 1.0 and 0.8 mg/ml for DLD-1, HCT116, SW480, SW620 and H1299 cells, respectively) for 2 weeks. Numbers of colonies generated were quantified using the Image J software. (**d**) Twenty-four hours after the transfection with pcDNA3.1+/XEDAR or mock plasmid, HEK293 cells were seeded in a poly-2-hydroxyethyl methacrylate-coated plate. The viability, caspase-3 activity and FAK expression in the cells were analyzed after the 24-h incubation. Results are given as ratio against the cells transfected with mock plasmid. β-Actin was used for the normalization of the expression levels. $^*P<0.05$ by Student's *t*-test.

failed to clarify the role of XEDAR in development. In this study, we showed the crucial role of the p53/XEDAR pathway in human carcinogenesis.

The X-linked ectodermal dysplasia receptor (XEDAR) interacts with TRAF3 and TRAF6, activates NF-κB signaling and consequently promotes cell proliferation

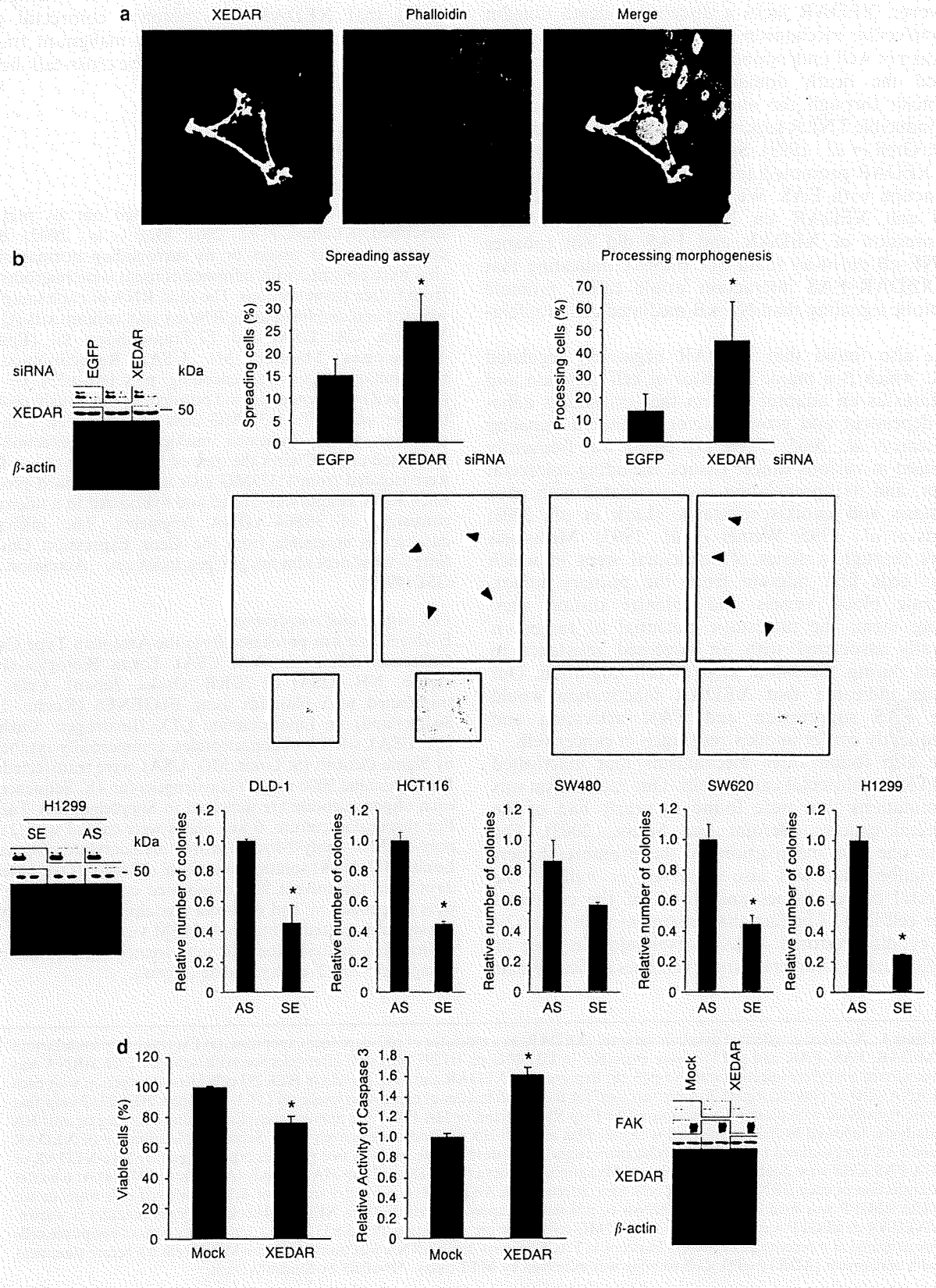

(Sinha *et al.*, 2002). On the other hand, the EDA-A2/XEDAR pathway was also shown to promote apoptotic cell death through the DISC (death-inducing signaling complex) formation containing FADD, caspase-8, caspase-10 and c-FLIP (Sinha and Chaudhary, 2004). However, XEDAR lacks a discernible death domain; the molecular mechanism of XEDAR-induced apoptosis was not well understood. Some TNFR members that lacked the death domain were shown to induce apoptosis through the interaction with FAS, another p53-inducible TNFR superfamily member (Afford *et al.*, 1999; Grell *et al.*, 1999). Similarly, our result suggested that XEDAR promoted apoptotic signaling through the interaction with FAS. We also examined the effect of FAS and XEDAR on NF-κB signaling; however, coexpression of XEDAR and FAS did not enhance the NF-κB pathway (data not shown), indicating that the XEDAR–FAS interaction would rather promote apoptotic signaling than NF-κB-mediated cell proliferation.

We also found that XEDAR negatively regulated FAK, which is a major mediator of cell adhesion and functions as an adaptor protein that transduces adhesion-dependent and growth factor-dependent signaling (McLean *et al.*, 2005). FAK expression was frequently increased in various cancer tissues, including colorectal cancer, and its upregulation was associated with poor prognosis and anoikis resistance (Lark *et al.*, 2003; Owens *et al.*, 1995; Weiner *et al.*, 1993). Metastasis occurs through a series of sequential steps in which tumor cells first migrate from the primary tumor, penetrate blood vessels and colonize distant sites. Among them, the metastatic potential of tumors is generally associated with an increased resistance to anoikis during the initial step of cell migration. Our findings indicated that XEDAR inactivation would cause FAS suppression and FAK activation and subsequently confer anoikis resistance in cancer cells.

We also found three mechanisms that inactivated XEDAR in colorectal cancer cells. One mechanism was *p53* mutations that were found in nearly half of the colorectal cancers (Beroud and Soussi, 2003). The second one was inactivation by the promoter hypermethylation that was also observed in half of the colorectal cancer tissues and in all of the colorectal cancer cell lines. The fact that treatment with 5-aza-2′-deoxycytidine restored *XEDAR* expression in none of the p53 mutant colorectal cancer cell lines indicated that either the p53 mutation or promoter hypermethylation is sufficient to suppress the *XEDAR* expression. In addition, we found, although rare, genetic mutations that would cause the inactivation of XEDAR in colorectal cancers. Taken together, our findings indicated that XEDAR is a putative colorectal tumor suppressor that would prevent the malignant transformation and tumor progression by the cross-talk between FAS and FAK.

Materials and methods

cDNA microarray

cDNA microarray analysis was carried out as previously described (Kitahara *et al.*, 2001; Mori *et al.*, 2002). Briefly, colorectal cancer tissues or its surrounding normal mucosa that were obtained with informed consent were microdissected from frozen tissue sections. The total RNA of each sample was isolated and amplified using RNeasy spin column kits (Qiagen, Valencia, CA, USA) and T7-Transcription kit (Epicentre Technologies, Madison, MI, USA). Replication-deficient recombinant adenovirus encoding p53 (Ad-p53) or LacZ (Ad-LacZ) was generated and purified, as previously described (Oda *et al.*, 2000). U373MG cells were infected with viral solutions at an indicated multiplicity of infection and incubated at 37 °C until the time of harvest. poly(A)+ RNAs were isolated from U373MG cells using a standard protocol. Each RNA sample was labeled and hybridized to a microarray consisting of 36 864 cDNA fragments. The microarray data set is accessible from the Gene Expression Omnibus (http://www.ncbi.nlm.nih.gov/geo/index.cgi, Accession No. GSE14953).

Cell culture and transfections

Each cell line was purchased from the American Type Culture Collection (Manassas, VA, USA), Lonza Biologics (Portsmouth, NH, USA) or JCRB (Osaka, Japan). Cells were transfected with plasmids using FuGENE6 (Roche, Basel, Switzerland) or Lipofectamine LTX (Invitrogen, Carlsbad, CA, USA). siRNA oligonucleotides, commercially synthesized by Sigma Genosis (St Louis, MO, USA), were transfected with Lipofectamine 2000 reagent (Invitrogen) for 4 h. Sequences for each oligonucleotide are indicated in Supplementary Table 1. For suspension culture, 6-well plates were coated with 2 ml of poly-HEMA (poly-2-hydroxyethyl methacrylate; Sigma, St Louis, MO, USA) solution in ethanol (10 mg/ml) for at least 3 days until the solvent had evaporated completely. The cells were suspended in 2 ml of media containing 0.5% methylcellulose and plated onto poly-HEMA-coated dishes. For methylation analysis, the cells were treated with an indicated dosage of 5-aza-2′-deoxycytidine (Sigma).

Figure 4 X-linked ectodermal dysplasia receptor (XEDAR) as a mediator of p53-dependent apoptosis. (**a**) Expressions of endogenous XEDAR, FAS, FAK and $p21^{WAF1}$ were examined in U373MG or H1299 cells 48 h after infection with Ad-p53. Each siRNA was transfected 6 h before infection with Ad-p53. (**b**) Expression of XEDAR and FAS protein in HEK293 cells after transfection with each siRNA (left) or plasmid (right). β-Actin was used for the normalization of expression levels. (**c**) Cell lysates from HEK293T cells that were transfected with plasmids expressing either Flag-XEDAR and/or HA-FAS were immunoprecipitated using anti-Flag or anti-HA antibody, followed by immunoblotting with anti-Flag and anti-HA antibody, respectively (left). Subcellular localization of XEDAR and FAS was examined by immunocytochemistry (right). Cells were transfected with two plasmids expressing either Myc-XEDAR or HA-FAS. Cells were double stained with anti-Myc antibody (Alexa fluor 488) and anti-HA antibody (Alexa fluor 594). (**d**) At 6 h after transfection of each siRNA, U373MG cells were infected with Ad-p53. Representative images of Ad-p53 infected cells were shown (left). siEGFP was used as control. Analysis of p53-induced apoptotic cell death in XEDAR knockdown cells (middle) is shown. siXEDAR or siEGFP was transfected into U373MG cells 6 h before infection with Ad-p53 or Ad-LacZ. Proportions of apoptotic cells are indicated as a percentage of sub-G1 fractions in FACS analysis. Each siRNA was transfected into MCF7 cells 6 h before treatment with adriamycin (ADR) (right). Cell viability was examined by MTT assay. $^*P<0.05$ by Student's *t*-test.

Quantitative real-time PCR

Quantitative real-time PCR was conducted using the SYBR Green I Master or Probe Master on a LightCycler 480 (Roche). The primer and probe sequences are indicated in Supplementary Table 1. The mRNA of 26 normal tissues was purchased from TAKARA Clontech (Kyoto, Japan).

ChIP assay

Chromatin immunoprecipitation assay was carried out using the CHIP Assay kit (Upstate Biotechnology, Waltham, MA, USA) as previously described (Tanikawa *et al*., 2003). PCR amplifications of *XEDAR* intron 1, containing the consensus p53-binding sites, were performed on immunoprecipitated

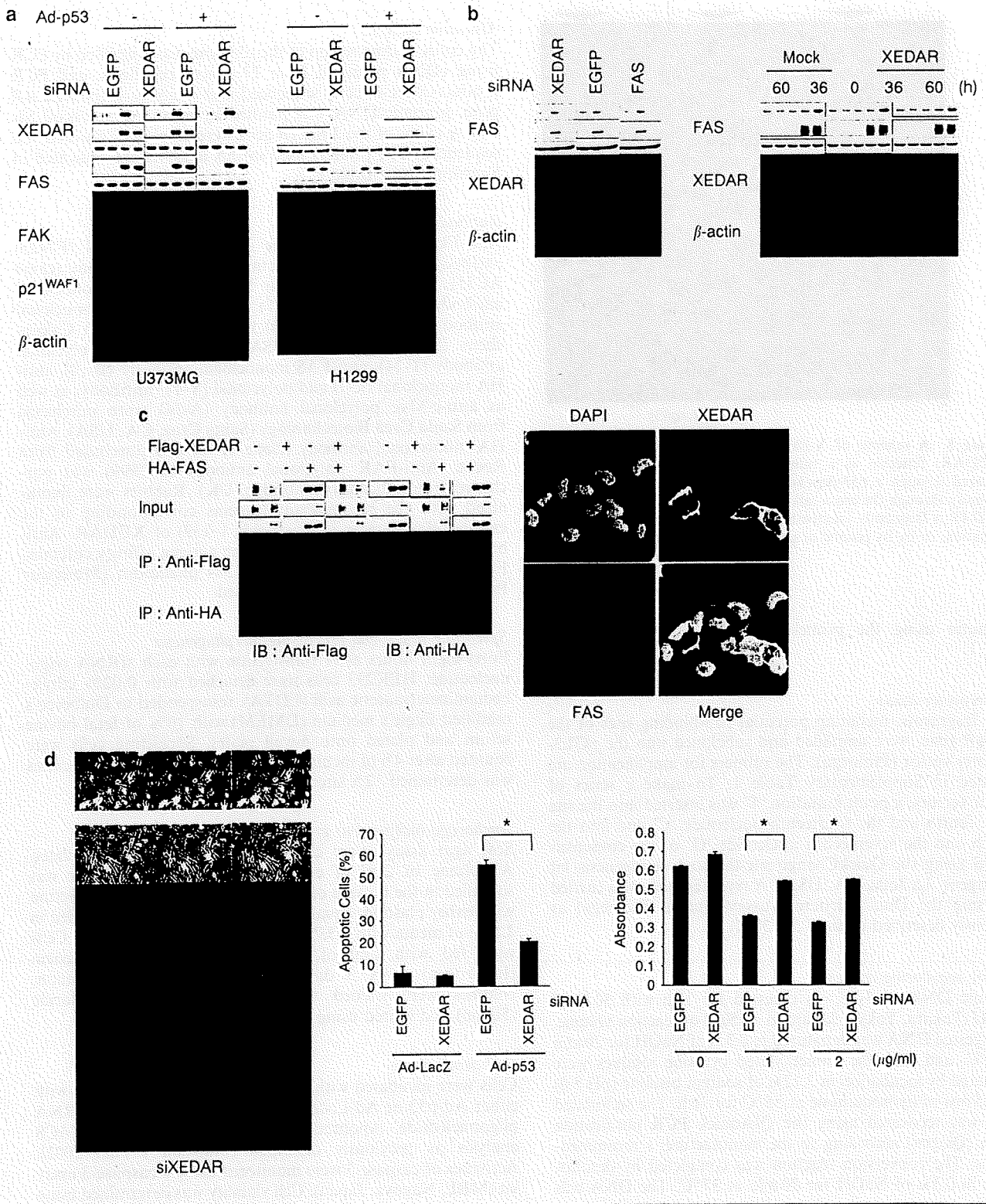

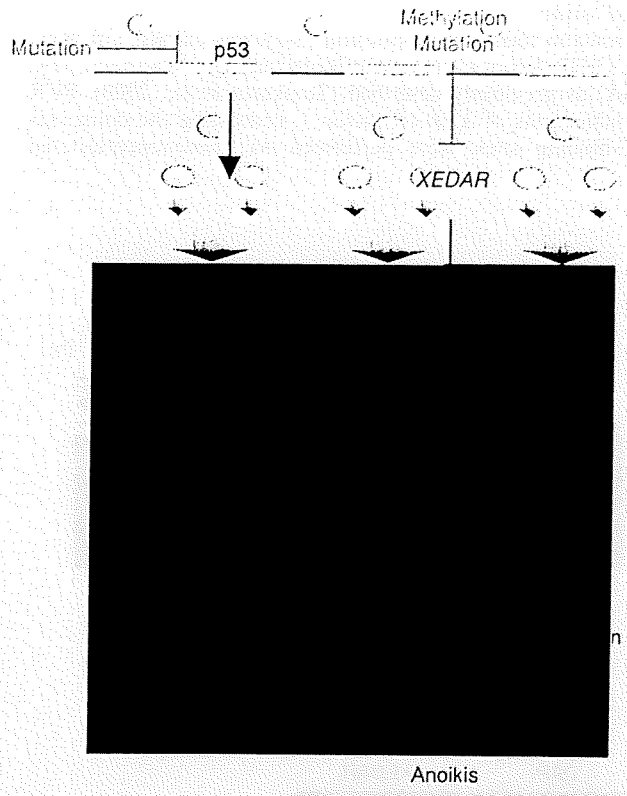

Figure 5 A schema of X-linked ectodermal dysplasia receptor (XEDAR) function as a tumor suppressor gene. *XEDAR* was induced through a p53-dependent manner and mediated anoikis pathway through the cross-talk between FAS and FAK. However, *XEDAR* is frequently inactivated in colorectal cancers by the *p53* mutation, or by its genetic or epigenetic alterations.

chromatin using the primers indicated in Supplementary Table 1.

Gene reporter assay

DNA fragments, including potential p53-binding sites of the *XEDAR* gene, were amplified and subcloned into the pGL3-promoter vector (Promega). The primers for amplification are indicated in Supplementary Table 1. To make a series of mutant vectors, a point mutation 'T' was inserted into the site of the fourth and the fourteenth nucleotide 'C' and into the seventh and the seventeenth nucleotide 'G' of the consensus p53-BS using the QuickChange site-directed mutagenesis kit (Stratagene, La Jolla, CA, USA). A reporter assay was carried out using the Dual Luciferase assay system (Promega) as previously described (Oda *et al*., 2000).

Bisulfite sequencing analysis

Genomic DNA of 3 μg was digested for 16 h with 30 U of *Sau3AI* (Takara, Tokyo, Japan) in a 150 μl of reaction volume. The digested DNA was denatured in 0.3 M of NaOH for 20 min at 37 °C, and then the unmethylated cytosine residues were sulfonated by incubation in 3.12 M of sodium bisulfite (pH 5.0) and 0.5 mM of hydroquinone at 55 °C for 16 h. The sulfonated DNA was recovered using the QIAquick PCR purification system (Qiagen) according to the manufacturer's recommendations. The conversion reaction was completed by desulfonating in 0.3 M of NaOH for 20 min at 37 °C. The DNA was ethanol precipitated and resuspended in double-distilled water. The modified DNA was subjected to PCR amplification of the CpG islands in the *XEDAR* promoter using the primers indicated in Supplementary Table 1. Amplified products were subcloned using the TOPO-TA Cloning System (Invitrogen). Plasmid DNA of at least six insert-positive clones was isolated and sequenced using the ABI sequencing system (Applied Biosystems, Foster City, CA, USA).

Mutation analysis

The entire coding region of the *p53* gene was amplified by PCR using cDNA prepared from 77 cancer cell lines, and PCR products were directly sequenced. For analysis in the *XEDAR* gene, genomic DNA was purified by standard protocol. Six coding exons of the *XEDAR* gene were amplified, purified and sequenced. The primers used in this analysis are indicated in Supplementary Table 1.

Antibodies

Anti-Flag monoclonal (clone M2) and polyclonal (F7425) antibody, as well as anti-β-actin monoclonal antibody (clone AC15) were purchased from Sigma. Anti-p53 monoclonal antibody (Ab-12, clone DO-7) and anti-$p21^{WAF1}$ monoclonal antibody (Ab-1, clone EA10) were purchased from Calbiochem (San Diego, CA, USA). Anti-XEDAR polyclonal antibody (T-14), anti-FAS monoclonal antibody (B-10), anti-HA monoclonal (F-7) and polyclonal (Y-11) antibody, as well as anti-c-Myc polyclonal antibody (A-14) were purchased from Santa Cruz Biotechnology (Santa Cruz, CA, USA). Anti-HA monoclonal antibody (clone 3F10) was purchased from Roche. Anti-FAK polyclonal antibody (ab2999) was purchased from Abcam (Cambridge, UK). Rabbits were immunized with the recombinant proteins corresponding to the extracellular domain (amino acids 1–139) of XEDAR. Antibodies were subsequently purified on antigen affinity columns. For labeling F-actin, Alexa fluor 594 phalloidin (Molecular Probes, Eugene, OR, USA) was used.

Spreading assay and processing morphogenesis

Forty-eight hours after transfection with each siRNA oligonucleotide, HEK293 cells were detached with 0.02% ethylenediaminetetraacetic acid (EDTA), resuspended in Dulbecco's modified Eagle's medium (DMEM) with 10% of fetal bovine serum and plated onto 6-well plates. Spreading cells were counted after 4 h of incubation, and processing morphogenesis was determined 12 h later.

Anchorage-independent growth assay

Soft agar assays were carried out in 6-well culture plates. A volume of 2 ml of culture media with 0.5% agar was solidified in the bottom of each well. At 24 h after transfection with either plasmid, equal numbers of cells were suspended in 1.5 ml of media with 0.33% agar and added to each well. Cells were fed with 1 ml of media supplement with geneticin (Invitrogen) every 3 days. After 2 weeks of incubation, colonies were stained with iodonitrotetrazolium chloride (Sigma) and scored using the Image J software.

Cell death assay

Cells were incubated with adriamycin for 2 h or infected with either Ad-p53 or Ad-LacZ at 6 h after transfection of siRNA oligonucleotide. Apoptotic cells were quantified by FACS analysis as previously described (Matsuda *et al*., 2002). Activities of caspase-3 were monitored using a caspase-3 assay kit (MBL, Nagoya, Japan). Cell viability was determined using

the MTT assay using Cell Counting Kit-8 (Dojindo, Kumamoto, Japan).

Conflict of interest

The authors declare no conflict of interest.

Acknowledgements

We thank T Katagiri for helpful discussion and A Takahashi K Makino for her technical assistance. This work was supported partly by grant #18687012 from Japan Society for the Promotion of Science and Ministry of education, culture, sports, science and technology of Japan (to KM). CT is a JSPS Research Fellow.

References

Afford SC, Randhawa S, Eliopoulos AG, Hubscher SG, Young LS, Adams DH. (1999). CD40 activation induces apoptosis in cultured human hepatocytes via induction of cell surface fas ligand expression and amplifies fas-mediated hepatocyte death during allograft rejection. *J Exp Med* **189**: 441–446.

Beroud C, Soussi T. (2003). The UMD-p53 database: new mutations and analysis tools. *Hum Mutat* **21**: 176–181.

Diez M, Medrano M, Muguerza JM, Ramos P, Hernandez P, Villeta R *et al.* (2000). Influence of tumor localization on the prognostic value of P53 protein in colorectal adenocarcinomas. *Anticancer Res* **20**: 3907–3912.

Folkman J, Moscona A. (1978). Role of cell shape in growth control. *Nature* **273**: 345–349.

Furutani M, Arii S, Tanaka H, Mise M, Niwano M, Harada T *et al.* (1997). Decreased expression and rare somatic mutation of the CIP1/WAF1 gene in human hepatocellular carcinoma. *Cancer Lett* **111**: 191–197.

Golubovskaya VM, Finch R, Kweh F, Massoll NA, Campbell-Thompson M, Wallace MR *et al.* (2008). p53 regulates FAK expression in human tumor cells. *Mol Carcinog* **47**: 373–382.

Grell M, Zimmermann G, Gottfried E, Chen CM, Grunwald U, Huang DC *et al.* (1999). Induction of cell death by tumour necrosis factor (TNF) receptor 2, CD40 and CD30: a role for TNF-R1 activation by endogenous membrane-anchored TNF. *EMBO J* **18**: 3034–3043.

Hollstein M, Rice K, Greenblatt MS, Soussi T, Fuchs R, Sorlie T *et al.* (1994). Database of p53 gene somatic mutations in human tumors and cell lines. *Nucleic Acids Res* **22**: 3551–3555.

Ilic D, Almeida EA, Schlaepfer DD, Dazin P, Aizawa S, Damsky CH. (1998). Extracellular matrix survival signals transduced by focal adhesion kinase suppress p53-mediated apoptosis. *J Cell Biol* **143**: 547–560.

Ilic D, Furuta Y, Kanazawa S, Takeda N, Sobue K, Nakatsuji N *et al.* (1995). Reduced cell motility and enhanced focal adhesion contact formation in cells from FAK-deficient mice. *Nature* **377**: 539–544.

Kidokoro T, Tanikawa C, Furukawa Y, Katagiri T, Nakamura Y, Matsuda K. (2008). CDC20, a potential cancer therapeutic target, is negatively regulated by p53. *Oncogene* **27**: 1562–1571.

Kitahara O, Furukawa Y, Tanaka T, Kihara C, Ono K, Yanagawa R *et al.* (2001). Alterations of gene expression during colorectal carcinogenesis revealed by cDNA microarrays after laser-capture microdissection of tumor tissues and normal epithelia. *Cancer Res* **61**: 3544–3549.

Lark AL, Livasy CA, Calvo B, Caskey L, Moore DT, Yang X *et al.* (2003). Overexpression of focal adhesion kinase in primary colorectal carcinomas and colorectal liver metastases: immunohistochemistry and real-time PCR analyses. *Clin Cancer Res* **9**: 215–222.

Lee SH, Shin MS, Kim HS, Lee HK, Park WS, Kim SY *et al.* (1999). Alterations of the DR5/TRAIL receptor 2 gene in non-small cell lung cancers. *Cancer Res* **59**: 5683–5686.

Levine AJ. (1997). p53, the cellular gatekeeper for growth and division. *Cell* **88**: 323–331.

Liang F, Liang J, Wang WQ, Sun JP, Udho E, Zhang ZY. (2007). PRL3 promotes cell invasion and proliferation by down-regulation of Csk leading to Src activation. *J Biol Chem* **282**: 5413–5419.

Liu X, Yue P, Khuri FR, Sun SY. (2005). Decoy receptor 2 (DcR2) is a p53 target gene and regulates chemosensitivity. *Cancer Res* **65**: 9169–9175.

Matsuda K, Yoshida K, Taya Y, Nakamura K, Nakamura Y, Arakawa H. (2002). p53AIP1 regulates the mitochondrial apoptotic pathway. *Cancer Res* **62**: 2883–2889.

McLean GW, Carragher NO, Avizienyte E, Evans J, Brunton VG, Frame MC. (2005). The role of focal-adhesion kinase in cancer—a new therapeutic opportunity. *Nat Rev Cancer* **5**: 505–515.

Mori T, Anazawa Y, Iiizumi M, Fukuda S, Nakamura Y, Arakawa H. (2002). Identification of the interferon regulatory factor 5 gene (IRF-5) as a direct target for p53. *Oncogene* **21**: 2914–2918.

Naito A, Yoshida H, Nishioka E, Satoh M, Azuma S, Yamamoto T *et al.* (2002). TRAF6-deficient mice display hypohidrotic ectodermal dysplasia. *Proc Natl Acad Sci USA* **99**: 8766–8771.

Nakamura Y. (2004). Isolation of p53-target genes and their functional analysis. *Cancer Sci* **95**: 7–11.

Newton K, French DM, Yan M, Frantz GD, Dixit VM. (2004). Myodegeneration in EDA-A2 transgenic mice is prevented by XEDAR deficiency. *Mol Cell Biol* **24**: 1608–1613.

Nikiforov MA, Hagen K, Ossovskaya VS, Connor TM, Lowe SW, Deichman GI *et al.* (1996). p53 modulation of anchorage independent growth and experimental metastasis. *Oncogene* **13**: 1709–1719.

Oda K, Arakawa H, Tanaka T, Matsuda K, Tanikawa C, Mori T *et al.* (2000). p53AIP1, a potential mediator of p53-dependent apoptosis, and its regulation by Ser-46-phosphorylated p53. *Cell* **102**: 849–862.

Owens LV, Xu L, Craven RJ, Dent GA, Weiner TM, Kornberg L *et al.* (1995). Overexpression of the focal adhesion kinase (p125FAK) in invasive human tumors. *Cancer Res* **55**: 2752–2755.

Pharoah PD, Day NE, Caldas C. (1999). Somatic mutations in the p53 gene and prognosis in breast cancer: a meta-analysis. *Br J Cancer* **80**: 1968–1973.

Rampino N, Yamamoto H, Ionov Y, Li Y, Sawai H, Reed JC *et al.* (1997). Somatic frameshift mutations in the BAX gene in colon cancers of the microsatellite mutator phenotype. *Science* **275**: 967–969.

Sinha SK, Chaudhary PM. (2004). Induction of apoptosis by X-linked ectodermal dysplasia receptor via a caspase 8-dependent mechanism. *J Biol Chem* **279**: 41873–41881.

Sinha SK, Zachariah S, Quinones HI, Shindo M, Chaudhary PM. (2002). Role of TRAF3 and -6 in the activation of the NF-kappa B and JNK pathways by X-linked ectodermal dysplasia receptor. *J Biol Chem* **277**: 44953–44961.

Smahi A, Courtois G, Rabia SH, Doffinger R, Bodemer C, Munnich A *et al.* (2002). The NF-kappaB signalling pathway in human diseases: from incontinentia pigmenti to ectodermal dysplasias and immune-deficiency syndromes. *Hum Mol Genet* **11**: 2371–2375.

Takakuwa T, Dong Z, Nakatsuka S, Kojya S, Harabuchi Y, Yang WI *et al.* (2002). Frequent mutations of Fas gene in nasal NK/T cell lymphoma. *Oncogene* **21**: 4702–4705.

Tanaka H, Arakawa H, Yamaguchi T, Shiraishi K, Fukuda S, Matsui K *et al.* (2000). A ribonucleotide reductase gene involved in

a p53-dependent cell-cycle checkpoint for DNA damage. *Nature* **404**: 42–49.

Tanikawa C, Matsuda K, Fukuda S, Nakamura Y, Arakawa H. (2003). p53RDL1 regulates p53-dependent apoptosis. *Nat Cell Biol* **5**: 216–223.

Vogelstein B, Fearon ER, Kern SE, Hamilton SR, Preisinger AC, Nakamura Y *et al*. (1989). Allelotype of colorectal carcinomas. *Science* **244**: 207–211.

Vogelstein B, Lane D, Levine AJ. (2000). Surfing the p53 network. *Nature* **408**: 307–310.

Weiner TM, Liu ET, Craven RJ, Cance WG. (1993). Expression of focal adhesion kinase gene and invasive cancer. *Lancet* **342**: 1024–1025.

Wu GS, Burns TF, McDonald III ER, Jiang W, Meng R, Krantz ID *et al*. (1997). KILLER/DR5 is a DNA damage-inducible p53-regulated death receptor gene. *Nat Genet* **17**: 141–143.

Yan M, Wang LC, Hymowitz SG, Schilbach S, Lee J, Goddard A *et al*. (2000). Two-amino acid molecular switch in an epithelial morphogen that regulates binding to two distinct receptors. *Science* **290**: 523–527.

Supplementary Information accompanies the paper on the Oncogene website (http://www.nature.com/onc)

Vol 461|10 September 2009|doi:10.1038/nature08283

ARTICLES

An RNA-dependent RNA polymerase formed by TERT and the *RMRP* RNA

Yoshiko Maida[1], Mami Yasukawa[1], Miho Furuuchi[1], Timo Lassmann[2], Richard Possemato[3], Naoko Okamoto[1], Vivi Kasim[1], Yoshihide Hayashizaki[2], William C. Hahn[3,4] & Kenkichi Masutomi[1,5]

Constitutive expression of telomerase in human cells prevents the onset of senescence and crisis by maintaining telomere homeostasis. However, accumulating evidence suggests that the human telomerase reverse transcriptase catalytic subunit (TERT) contributes to cell physiology independently of its ability to elongate telomeres. Here we show that TERT interacts with the RNA component of mitochondrial RNA processing endoribonuclease (*RMRP*), a gene that is mutated in the inherited pleiotropic syndrome cartilage–hair hypoplasia. Human TERT and *RMRP* form a distinct ribonucleoprotein complex that has RNA-dependent RNA polymerase (RdRP) activity and produces double-stranded RNAs that can be processed into small interfering RNA in a Dicer (also known as DICER1)-dependent manner. These observations identify a mammalian RdRP composed of TERT in complex with *RMRP*.

Telomerase is a ribonucleoprotein complex that elongates telomeres. Although several proteins interact with telomerase[1–4], the minimal components of active telomerase include the catalytic telomerase reverse transcriptase (TERT) and a noncoding RNA (*TERC*) that encodes the template to synthesize telomeric DNA[5]. Telomere homeostasis mediated by telomerase maintains genomic stability and regulates cell lifespan[6]. Mutations in TERT, *TERC* or dyskerin, a telomerase-associated nucleolar protein involved in ribosomal RNA maturation[7], are found in dyskeratosis congenita, a syndrome characterized by ectodermal dysplasia and bone marrow failure, and TERT mutations have been reported in aplastic anaemia and idiopathic pulmonary fibrosis[8]. Moreover, alterations in the regulation of telomeres and telomerase contribute to malignant transformation by affecting genomic integrity and cell immortalization[9].

However, accumulating evidence suggests that TERT has activities beyond telomere maintenance[9–13] and forms several intracellular complexes[2–4]. In particular, the overexpression of TERT induces increased tumour susceptibility[9,10] and disrupts stem-cell function independently of telomere maintenance[12], whereas the suppression of TERT expression alters global chromatin structure[11]. Indeed, some of these telomere-independent functions of TERT do not require the expression of *TERC*[12].

Identification of a second RNA that interacts with TERT

To identify human TERT partners, we stably overexpressed a tandem affinity peptide (TAP)-tagged TERT protein in HeLa S3 cells, isolated TERT immune complexes, and identified a heterogeneous mixture of 38 RNA sequences associated with TERT (Supplementary Fig. 2 and Supplementary Table 1). We found that 5% of the sequences corresponded to *TERC* and the RNA component of mitochondrial RNA processing endoribonuclease (*RMRP*). *RMRP* is a 267-nucleotide noncoding RNA that is a small nucleolar RNA, like *TERC*, and is also found in mitochondria[8,14]. *RMRP* mutations are found in the pleiotropic inherited syndrome, cartilage–hair hypoplasia[15].

From a single immune complex, we confirmed that either overexpressed or endogenous TERT interacts with *RMRP* and *TERC*, by isolating TAP–TERT (Fig. 1a) or endogenous TERT (Fig. 1b) complexes in both HeLa and 293T cells under conditions in which we failed to recover the ribozyme *RNase P*. We also found that the abundance of TERT–*RMRP* and TERT–*TERC* complexes was similar, even though *TERC* was expressed at five-fold higher levels than *RMRP* in these cells (Fig. 1c and Supplementary Fig. 3).

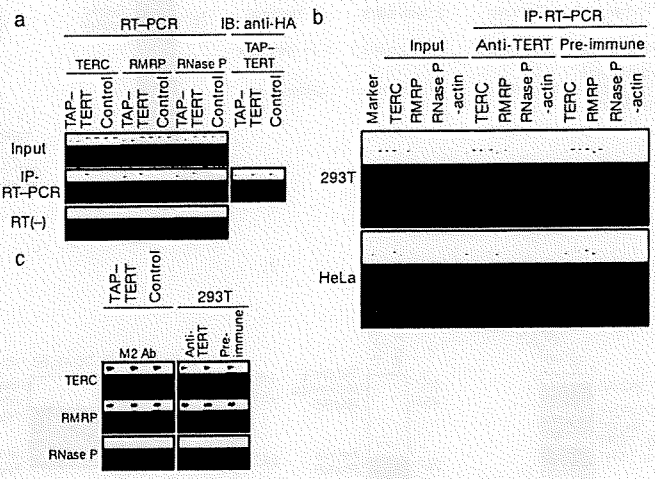

Figure 1 | TERT and *RMRP* interact. **a**, Detection of *RMRP* and *TERC* RNA species associated with TAP–TERT complexes from a single immunoprecipitation (IP) were isolated and subjected to PCR with reverse transcription (RT–PCR). RT (−) indicates the absence of reverse transcriptase. Right panel shows the levels of TAP–TERT. HA, haemagglutinin; IB, immunoblot. **b**, TERT interacts with endogenous *RMRP*. TERT complexes from 293T and HeLa cells were isolated with an anti-TERT antibody and associated RNAs were subjected to RT–PCR. **c**, RNAs purified from TERT complexes isolated from HeLa S3 cells expressing TAP–TERT or a control vector or 293T cells were subjected to northern blotting. Ab, antibody.

[1]Cancer Stem Cell Project, National Cancer Center Research Institute, 5-1-1 Tsukiji, Chuo-ku, Tokyo 104-0045, Japan. [2]RIKEN Omics Science Center, RIKEN Yokohama Institute, 1-7-22 Suehiro-cho, Tsurumi-ku, Yokohama 230-0045, Japan. [3]Department of Medical Oncology, Dana-Farber Cancer Institute and Departments of Medicine, Brigham and Women's Hospital and Harvard Medical School, 44 Binney Street, Boston, Massachusetts 02115, USA. [4]Broad Institute of Harvard and MIT, 7 Cambridge Center, Cambridge, Massachusetts 02142, USA. [5]PREST, Japan Science and Technology Agency, 4-1-8 Honcho Kawaguchi, Saitama 332-0012, Japan.

To characterize the interaction between TERT and *RMRP*, we used TERT truncation mutants and found that the amino terminal end of TERT (1–531) was necessary for interactions with *RMRP* (Supplementary Fig. 4). This region overlaps with two regions required for the binding of *TERC*[8,16]. These observations demonstrate that TERT and *RMRP* form a new ribonucleoprotein complex distinct from the TERT–*TERC* enzyme.

The TERT–*RMRP* complex has RdRP activity

To test whether *RMRP* substitutes for *TERC* to reconstitute telomerase activity, we combined recombinant TERT with *TERC* or *RMRP* RNAs transcribed *in vitro*. Although we detected telomerase activity with TERT and *TERC* (Supplementary Fig. 5), we failed to detect telomerase activity when TERT and *RMRP* were co-incubated.

TERT has also been shown to act as a terminal transferase[17], and human TERT shares sequence similarity to both viral reverse transcriptases and RdRPs[18]. RdRPs participate in the endogenous RNA interference (RNAi) pathway and in the regulation of post-transcriptional gene silencing[19–23]. To examine whether the TERT–*RMRP* complex has RdRP and/or terminal transferase activity, we established an RNA synthesis activity assay with recombinant TERT protein (Supplementary Fig. 6) and RNA molecules transcribed *in vitro*. We predicted three modes that the TERT–*RMRP* complex might use to elongate RNA: (1) as an RdRP that uses a *de-novo*-synthesized RNA primer to elongate a complementary strand (Fig. 2a, left panel); (2) as an RdRP that uses a 3′ fold-back (back-priming) configuration of template RNA as a primer (Fig. 2a, middle panel); or (3) as a terminal transferase (Fig. 2a, right panel). Viral RdRPs[24,25] have been shown to use the first two modes to prime RdRP activity, and cellular RdRPs in fission yeast[26] and fungi[23] use similar priming mechanisms to produce double-stranded (ds) RNAs that act as precursors for RNAi.

We found that recombinant TERT and *RMRP* produced two different products depending on the salt concentration (Fig. 2b and Supplementary Fig. 7). Specifically, we found ~267-nucleotide-(corresponding to sense *RMRP*) and ~534-nucleotide-sized products (hereafter referred to as sense plus antisense *RMRP* products) under high salt conditions, and *RMRP*-sized products under low salt conditions. To discriminate between these modes, we treated the products of the RdRP assay with RNase T1 (Fig. 2c) using conditions that favour the digestion of single-stranded RNA. RNase T1 treatment eliminated the ~267-nucleotide *RMRP*-sized RNA products produced under low salt concentrations (data not shown), indicating that [^{32}P]UTP was incorporated by terminal transferase activity.

In contrast, under high salt conditions, we found two RNAs (~267 and ~534 nucleotides) that collapsed into a single ~267-nucleotide band after treatment with RNase T1 (Fig. 2c). To eliminate the possibility that the sense plus antisense product represented partially denatured RNAs, we treated the products of the RdRP assay with bacterial RNase III to digest dsRNA, and found that only the input ~267-nucleotide RNA remained (Fig. 2d). Furthermore, when we left out adenine or guanine ribonucleotides, we failed to detect the sense plus antisense product (Fig. 2e). These observations confirm that the ~534-nucleotide sense plus antisense products are formed by RdRP activity and represent a double-stranded hairpin structure created by an RNA molecule composed of sense and antisense strands of *RMRP*.

To confirm that the interaction between TERT and *RMRP* was required for RdRP activity, we performed an RdRP activity assay using

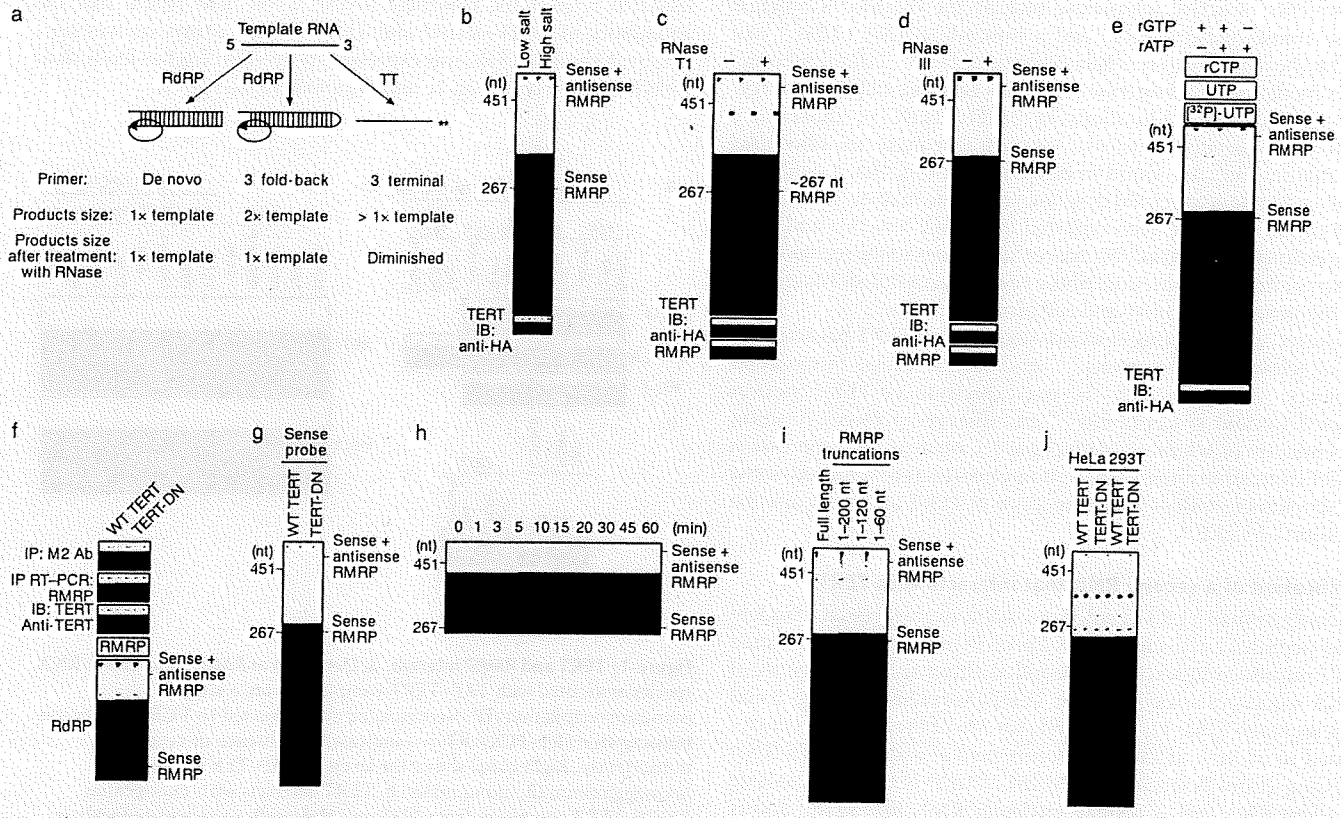

Figure 2 | TERT and *RMRP* have RdRP activity. **a**, Predicted RNA products produced by RdRP or terminal transferase (TT) activity. **b**, RNA products produced by the RdRP activity derived from recombinant TERT and *RMRP*. nt, nucleotides. **c**, **d**, Treatment of RNA products with RNase T1 (**c**) or bacterial RNase III (**d**). **e**, RdRP assay performed in the presence of ribonucleotides (middle) or in the absence of adenine (left lane) or guanine (right lane) ribonucleotides. A and G are present within the first 5 nucleotides of the predicted complementary strand of *RMRP*. **f**, TERT-DN binds *RMRP* but lacks RdRP activity. TERT immune complexes were isolated from 293T cells expressing Flag-tagged TERT or Flag-tagged TERT-DN. RdRP activity is shown in the bottom panel. WT, wild-type. **g**, Northern blotting to detect complementary sequence of *RMRP*. **h**, Time course of RdRP activity. **i**, RNA products produced by recombinant TERT and truncation mutants of *RMRP* transcribed *in vitro*. Faint signals at 200, 120 and 60 nucleotides are TERT terminal transferase products. **j**, RNA products produced by the RdRP activity derived from recombinant TERT or TERT-DN and total RNA. A limited pool of RNAs serves as template for RdRP activity.

combinations of recombinant mutant TERT proteins and *RMRP*. We failed to detect RdRP reaction products when TERT and *TERC* were co-incubated (Supplementary Fig. 8). Moreover, when we used the TERT-HT1 mutant that does not bind *RMRP* (Supplementary Fig. 4), we failed to observe labelled RNA products (Supplementary Fig. 8) under conditions in which we detected two different RNA products in reactions containing wild-type TERT and *RMRP*. We previously described a catalytically inactive TERT mutant (TERT-DN) that fails to elongate telomeres[11,27]. We confirmed that the recombinant TERT-DN mutant retained the ability to bind *RMRP* (Fig. 2f), but that the TERT-DN–*RMRP* complex lacked detectable RdRP activity (Fig. 2f). Thus TERT acts as the catalytic subunit for both the telomerase reverse transcriptase and RdRP activities.

TERT–*RMRP* RdRP produces dsRNA

These observations suggest that the TERT–*RMRP* RdRP synthesizes dsRNA in a template-dependent manner. To confirm the synthesis of the *RMRP* complementary strand, we used the sense strand of *RMRP* as a probe in northern blotting. We detected the antisense strand of *RMRP* in reactions containing recombinant wild-type TERT protein and *RMRP*, but not in reactions containing TERT-DN and *RMRP* (Fig. 2g). Furthermore, we detected the sense plus antisense product in the RdRP assay using the antisense strand of *RMRP* as a probe (Supplementary Fig. 9). These observations indicate that the TERT–*RMRP* RdRP produces dsRNAs in a template-dependent manner *in vitro*.

To determine whether the TERT–*RMRP* RdRP uses a back-priming mechanism, we examined the priming process using TERT and *RMRP* as a model system and found that elongation products appeared in a time-dependent manner (Fig. 2h and Supplementary Fig. 10). To assess whether the *RMRP* RNA forms a 3′ fold-back configuration, we generated 3′ *RMRP* truncation mutants and failed to find any reaction products (Fig. 2i). Thus, unlike what has been described for other cellular RdRPs, the TERT–*RMRP* RdRP has a restricted preference for RNA molecules that can be used as a template. Indeed, when we incubated purified recombinant TERT together with total cellular RNA and [^{32}P]UTP, we identified a limited number of labelled RNAs (Fig. 2j). Although the secondary structure adopted by *RMRP* to create the 3′ fold-back is not known, these observations suggest that *RMRP* can itself serve as a primer for the polymerization process using a 3′ fold-back structure.

To ascertain whether this RdRP activity also occurs *in vivo*, we used the sense strand of *RMRP* as a probe and found ~534-nucleotide RNAs that contain antisense *RMRP* in RNA derived from 293T, HeLa and MCF7 cells (Fig. 3a and Supplementary Figs 11 and 12). Moreover, we detected sense products and sense plus antisense products using *RMRP* antisense-strand probe (Fig. 3b). These observations confirmed that the ~534-nucleotide products contain both sense and antisense *RMRP* sequences. To determine whether TERT was necessary for the appearance of antisense *RMRP* in cells, we examined the levels of the complementary *RMRP* strand in cells that do not express TERT and *TERC* (VA-13 cells)[28], in cells that transiently express low levels of TERT (BJ cells)[27,29,30], and in cells that constitutively express TERT (293T and HeLa cells). We also introduced a control vector or a vector that encodes TERT in VA-13 and BJ cells. We detected the complementary *RMRP* strand using a quantitative RNase protection assay with a sense-strand probe that detects antisense *RMRP* (Fig. 3c and Supplementary Fig. 13), and using northern blotting with both sense and antisense strand-specific *RMRP* probes (Fig. 3d and Supplementary Fig. 11a). The levels of antisense *RMRP* correlated with the expression of TERT (Fig. 3c, d). These observations confirmed that the TERT–*RMRP* RdRP produces double-stranded *RMRP in vivo*.

Effects of the TERT–*RMRP* complex on *RMRP* expression

To assess the consequences of overexpressing the TERT–*RMRP* complex on *RMRP* levels, we introduced *RMRP* into cells that lack TERT

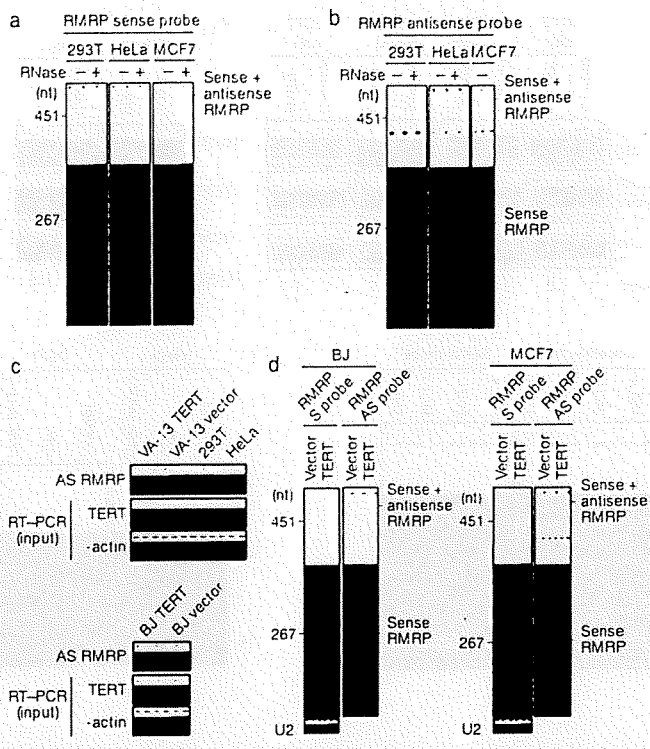

Figure 3 | Identification of dsRNA synthesized by the TERT–*RMRP* RdRP. **a**, Northern blotting to detect complementary sequence of *RMRP* in cell lines. '+' indicates samples treated with RNase. **b**, Northern blotting to detect the *RMRP* sense strand. **c**, TERT expression correlates with the levels of antisense (AS) *RMRP* detected by RNase protection assay. Vector denotes cells infected with a control vector. **d**, TERT expression correlates with the levels of the sense (S) plus antisense *RMRP* products detected by northern blotting. The bottom panel shows levels of the small nuclear RNA *U2*.

expression (VA-13), that transiently express TERT in a cell-cycle-dependent manner (BJ fibroblasts), and that constitutively express TERT (VA-13 and BJ fibroblasts expressing ectopic TERT, and HeLa and MCF7 cells). After expressing *RMRP* in cells lacking TERT (VA-13), we found that *RMRP* levels were increased (Fig. 4a and Supplementary Fig. 14). In contrast, in cells that express TERT, we found that the steady-state levels of *RMRP* were decreased when *RMRP* was overexpressed, regardless of the promoter that was used to express *RMRP* (Fig. 4a and Supplementary Fig. 14). We also found that forced TERT expression in VA-13 or BJ cells suppressed *RMRP* expression (Fig. 4b and Supplementary Fig. 15). Consistent with these findings, suppression of TERT in HeLa cells led to increased *RMRP* expression (Fig. 4c).

Because the 3′ end of *RMRP* was essential for TERT–*RMRP* activity (Fig. 2i), we examined the effects of expressing *RMRP* truncation mutants lacking 3′ ends and found that only truncation mutants lacking intact 3′ ends were readily overexpressed (Fig. 4d). These observations demonstrate that *RMRP* expression levels are dependent on the TERT–*RMRP* RdRP and suggest that *RMRP* levels are controlled by an RdRP-dependent, negative-feedback mechanism.

Identification of siRNAs derived from *RMRP*

In other organisms, RdRPs synthesize dsRNAs that are processed into active short interfering RNAs (siRNAs)[31]. Because manipulating TERT and *RMRP* levels affected *RMRP* expression, we proposed that the TERT–*RMRP* complex produces *RMRP*-specific siRNA to regulate *RMRP* levels. To test this possibility, we used sense and antisense probes corresponding to *RMRP* (nucleotides 21–40) in northern blotting and found double-stranded 22-nucleotide RNAs (Fig. 4e and Supplementary Fig. 11b). Because siRNAs contain 5′ monophosphate and 3′ hydroxyl groups[32–34], we characterized the chemical

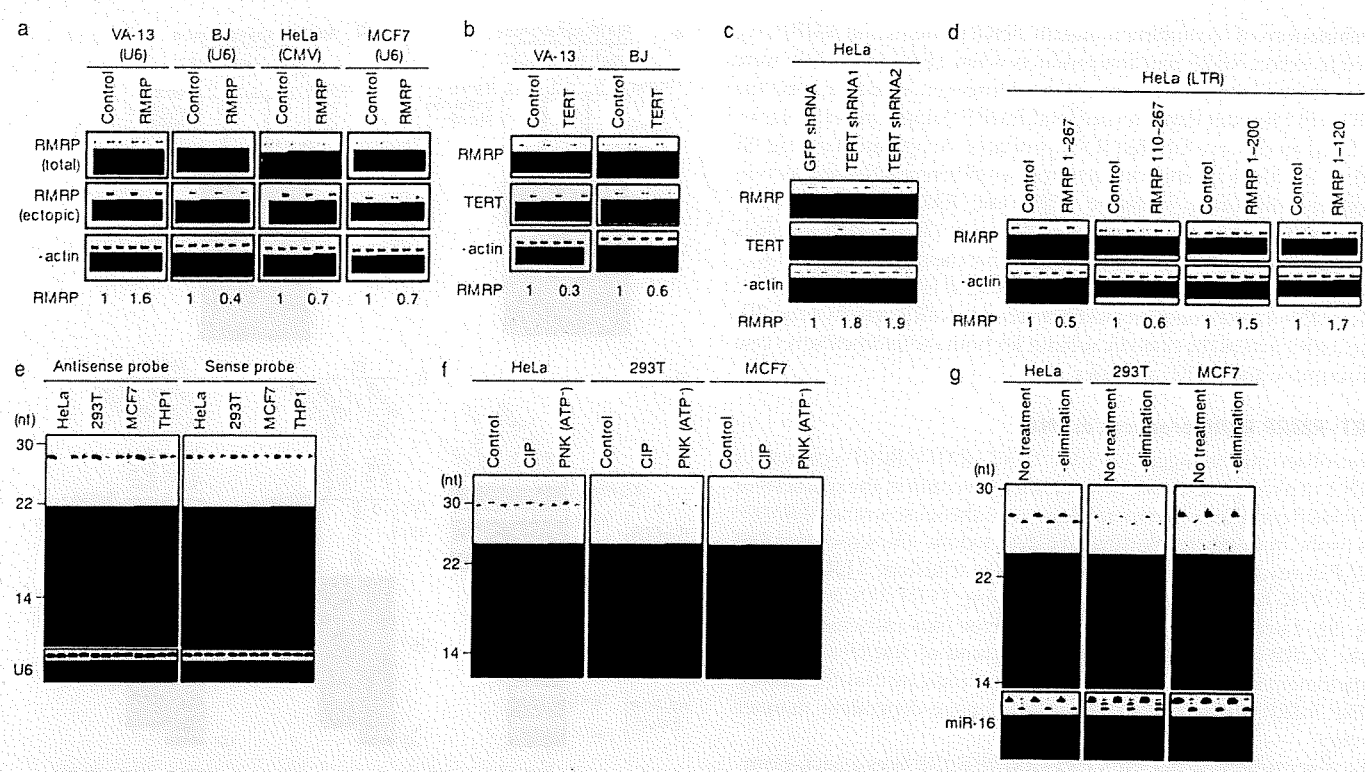

Figure 4 | Effects of dsRNA produced by the TERT–*RMRP* RdRP. a, Semi-quantitative RT–PCR for total *RMRP* and retrovirally delivered *RMRP* (ectopic) in cell lines expressing control or *RMRP* expression vectors. Promoters used to express *RMRP* are indicated. The relative intensity of *RMRP* is noted below each panel. CMV, cytomegalovirus. See Supplementary Fig. 14. **b**, RT–PCR for total *RMRP*. See Supplementary Fig. 15. **c**, Effects of suppressing TERT on *RMRP* levels. A control shRNA (green fluorescent protein (GFP) shRNA) or two different *TERT*-specific shRNAs were stably introduced into HeLa cells. **d**, Effects of *RMRP* mutants on *RMRP* levels. LTR, long terminal repeat. RT–PCR was used to detect *RMRP* levels in **c** and **d**. **e**, Detection of small RNA species in human cells. Northern blotting to detect small RNAs (22 nucleotides in length) using antisense (left panel) and sense (right panel) probes derived from nucleotides 21–40 of *RMRP*. **f**, **g**, Analysis of the termini of the small RNA species identified in **e**. Total RNA was incubated with the indicated enzyme (**f**), or oxidation-β-elimination reactions (**g**) were performed. Northern blotting was performed with antisense probe. CIP, calf intestinal phosphatase; PNK, polynucleotide kinase. ATP- indicates samples lacking ATP.

nature of the small RNA ends. We found that calf intestinal phosphatase slowed the migration of these short RNAs, and subsequent incubation with polynucleotide kinase and ATP restored the mobility of the short RNAs, indicating that either the 5′ or the 3′ end of this small RNA is monophosphorylated (Fig. 4f and data not shown). Moreover, incubation with polynucleotide kinase in the absence of ATP did not alter the migration (Fig. 4f), and oxidation and β-elimination treatment increased the migration of these small RNAs (Fig. 4g), indicating that the 3′ ends bear vicinal 2′,3′ dihydroxyls. Together, these observations confirm that these small RNAs contain 5′ monophosphate and 3′ hydroxyl groups, and therefore share the size and chemical composition of known siRNAs.

To demonstrate that dsRNAs produced by the TERT–*RMRP* RdRP are processed into siRNA, we suppressed the expression of *Dicer* with two distinct *Dicer*-specific short hairpin RNAs (shRNAs). Suppression of *Dicer* to levels that partially inhibited the processing of the microRNA *miR-16* (Fig. 5a and Supplementary Fig. 16) led to diminished levels of the siRNAs derived from *RMRP* (Fig. 5a). When we suppressed *Dicer* expression in HeLa, 293T or MCF7 cells, we found that endogenous *RMRP* levels increased up to 3.7-fold (Fig. 5b). Suppressing *Dicer* expression in VA-13 cells that lack TERT did not affect the levels of single-stranded *RMRP* (Fig. 5b), but did increase levels of the elongated sense plus antisense *RMRP* products in cells that constitutively express TERT (Supplementary Fig. 17). Moreover, we found that only the sense strands of these endogenous *RMRP*-specific siRNAs were associated with human AGO2 (also known as EIF2C2; Fig. 5c). These observations indicate that the endogenous *RMRP*-specific siRNAs are processed by the RNA-induced silencing complex, similar to other small RNAs that are processed into siRNA.

To confirm that these small RNAs act as siRNAs, we identified small RNAs from total RNA that hybridized to probes spanning *RMRP*, synthesized siRNA corresponding to the identified sequences, and tested the consequences of introducing this siRNA in HeLa, 293T and MCF7 cells. We found that the synthesized siRNA suppressed endogenous *RMRP* levels (Supplementary Fig. 18). These observations provide evidence that similar to other cellular RdRPs, the TERT–*RMRP* RdRP synthesizes dsRNAs that act as a precursor for siRNAs.

Discussion

Here we demonstrate that human TERT and *RMRP* form a distinct ribonucleoprotein complex that has the ability to produce dsRNAs (Supplementary Fig. 1). Like RdRPs found in other organisms, the human TERT–*RMRP* complex produces dsRNAs that act as substrates for the generation of siRNA. However, unlike other cellular RdRPs[23,26,31,35,36], the human TERT–*RMRP* RdRP shows a strong preference for RNA templates that can form 3′ fold-back structures. Because other cellular RdRPs have been identified using assays that require primer-independent RdRP activity[23,26,36], the substrate specificity of the human TERT–*RMRP* RdRP may, in part, account for the difficulty in identifying mammalian enzymes that have RdRP activity.

Although the cellular RdRPs described until now do not show a primer requirement, several viral RdRPs use both primer-dependent and primer-independent mechanisms, and fungal and yeast RdRPs are also able to use a back-priming mechanism[23,26]. Because TERT is a closed right-handed polymerase[37] evolutionarily related to both reverse transcriptases and viral RdRPs[18], these observations are consistent with previous observations that indicate that right-handed RdRPs exhibit primer-dependent RdRP polymerase activity[38].

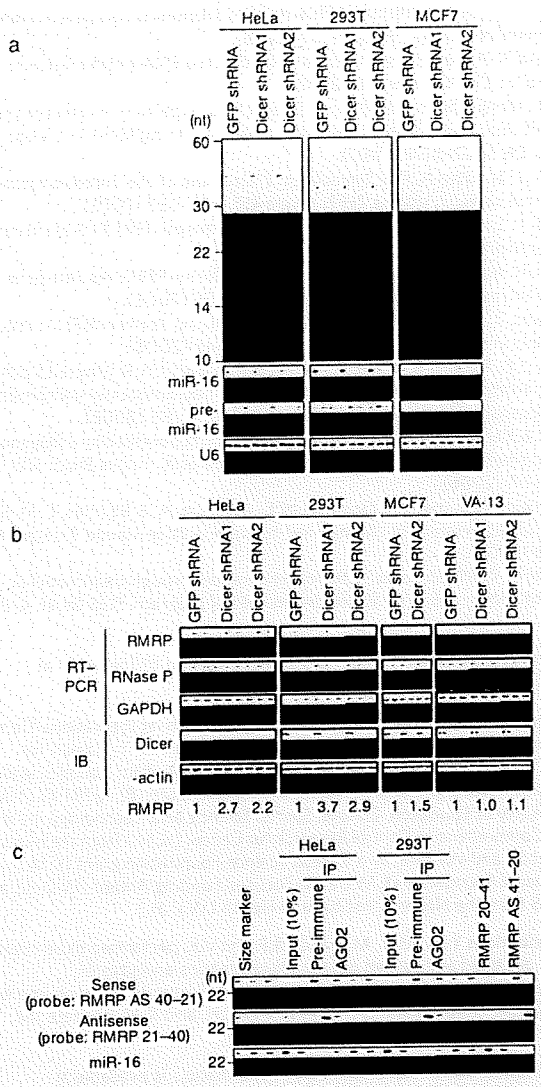

Figure 5 | Production of *RMRP*-derived endogenous siRNAs depends on Dicer. **a**, Effect of suppressing *Dicer* on *RMRP*-derived small RNAs. Northern blotting was performed to detect: (1) small RNAs using the antisense strand of *RMRP* as a probe in the indicated cells expressing control shRNA (GFP shRNA) or *Dicer*-specific shRNAs (*Dicer* shRNA1 and shRNA2); (2) precursor microRNA *pre-miR-16* and mature *miR-16* using a *miR-16*-specific probe; and (3) *U6* RNA. See Supplementary Fig. 16. **b**, RT–PCR for total *RMRP* from cell lines expressing control shRNA or *Dicer*-specific shRNAs. IB, immunoblot. The relative intensity of *RMRP* is noted at the bottom of the panel. **c**, *RMRP*-derived small RNAs are associated with AGO2. Human AGO2 immune complexes were isolated using anti-AGO2-specific antisera or pre-immune sera, and small RNAs were detected by northern blotting. Blotting of oligonucleotides (*RMRP* 20–41 and *RMRP* AS 41–20) is also shown.

Using *RMRP* as a template, the TERT–*RMRP* RdRP produces dsRNAs that are processed by Dicer into 22-nucleotide dsRNAs that contain 5′ monophosphate and 3′ hydroxyl groups and are loaded into AGO2, confirming that these short RNAs represent endogenous siRNAs. Recent work has shown that in oocytes and embryonic stem cells, endogenous siRNA can also be formed by the transcription of complementary sense and antisense strands[39–41]. Thus, in mammals at least two mechanisms lead to the production of dsRNAs that are processed into siRNA. Further work will be necessary to determine whether there are tissue-dependent differences in the use of these two mechanisms and whether other mammalian RdRPs exist.

We found that the TERT–*RMRP* RdRP regulates *RMRP* levels by a negative-feedback control mechanism. The identities and functions of the RNAs other than *RMRP* that act as templates for the TERT–*RMRP* RdRP remain to be identified (Fig. 2j). However, because endogenously encoded siRNAs suppress L1 retrotransposition in human cells[42], these observations suggest that the TERT–*RMRP* complex may regulate the expression of other genes by generating siRNAs.

Because mutations in *RMRP* are found in cartilage–hair hypoplasia[15], these findings suggest that perturbation of the TERT–*RMRP* complex is involved in the pathogenesis of this disorder. The involvement of human TERT in two syndromes characterized by stem-cell failure (cartilage–hair hypoplasia and dyskeratosis congenita)[7,8,43] suggests that ribonucleoprotein complexes containing TERT has a critical role in stem cell biology. Indeed, overexpression of mouse TERT in mice lacking *Terc* leads to defects in normal hair follicle stem-cell function[12] at least in part by altering gene expression programs related to stem cell function[44]. In mammals, TERT may regulate both telomere biology and gene expression through these two ribonucleoprotein complexes.

METHODS SUMMARY

RNAs that bind TERT were identified from HeLa S3 cells expressing a TAP epitope-tagged TERT. RNAs that bound to TERT after two rounds of purification were analysed using an Experion capillary electrophoresis device (Bio-Rad) to visualize RNA species. For RNA cloning and sequencing, the same samples were separated using a 7 M urea/15% polyacrylamide gel, and RNAs recovered from the gel were cloned using a small RNA cloning kit (TaKaRa). Purified glutathione *S*-transferase (GST)–TERT was isolated from *Escherichia coli* and incubated with either *TERC* or *RMRP* transcribed *in vitro*, to assess the ability of such complexes to exhibit telomerase or RdRP activity. RNAi was used to suppress TERT and to show that the TERT–*RMRP* complex also produces dsRNA in cells. Northern blotting with sense and antisense probes specific for *RMRP* (nucleotides 21–40) identified 22-nucleotide, double-stranded RNAs that contained a 5′ monophosphate and a 3′ hydroxyl group, which were loaded into human AGO2. To determine the function of these *RMRP*-derived small RNAs, a chemically synthesized siRNA corresponding to these small RNAs (siRNA: 5′-GGCTACACACTGAGGACTC-3′; Dharmacon) was transfected into HeLa, 293T and MCF7 cells.

Full Methods and any associated references are available in the online version of the paper at www.nature.com/nature.

Received 28 May; accepted 10 July 2009.
Published online 23 August 2009.

1. Cohen, S. B. *et al.* Protein composition of catalytically active human telomerase from immortal cells. *Science* 315, 1850–1853 (2007).
2. Fu, D. & Collins, K. Purification of human telomerase complexes identifies factors involved in telomerase biogenesis and telomere length regulation. *Mol. Cell* 28, 773–785 (2007).
3. Venteicher, A. S., Meng, Z., Mason, P. J., Veenstra, T. D. & Artandi, S. E. Identification of ATPases pontin and reptin as telomerase components essential for holoenzyme assembly. *Cell* 132, 945–971 (2008).
4. Venteicher, A. S. *et al.* A human telomerase holoenzyme protein required for Cajal body localization and telomere synthesis. *Science* 323, 644–648 (2009).
5. Weinrich, S. L. *et al.* Reconstitution of human telomerase with the template RNA component hTR and the catalytic protein subunit hTRT. *Nature Genet.* 17, 498–502 (1997).
6. Chan, S. W. & Blackburn, E. H. New ways not to make ends meet: telomerase, DNA damage proteins and heterochromatin. *Oncogene* 21, 553–563 (2002).
7. Liu, J. M. & Ellis, S. R. Ribosomes and marrow failure: coincidental association or molecular paradigm? *Blood* 107, 4583–4588 (2006).
8. Calado, R. T. & Young, N. S. Telomere maintenance and human bone marrow failure. *Blood* 111, 4446–4455 (2008).
9. Gonzalez-Suarez, E. *et al.* Increased epidermal tumors and increased skin wound healing in transgenic mice overexpressing the catalytic subunit of telomerase, mTERT, in basal keratinocytes. *EMBO J.* 20, 2619–2630 (2001).
10. Artandi, S. E. *et al.* Constitutive telomerase expression promotes mammary carcinomas in aging mice. *Proc. Natl Acad. Sci. USA* 99, 8191–8196 (2002).
11. Masutomi, K. *et al.* The telomerase reverse transcriptase regulates chromatin state and DNA damage responses. *Proc. Natl Acad. Sci. USA* 102, 8222–8227 (2005).
12. Sarin, K. Y. *et al.* Conditional telomerase induction causes proliferation of hair follicle stem cells. *Nature* 436, 1048–1052 (2005).
13. Lee, J. *et al.* TERT promotes cellular and organismal survival independently of telomerase activity. *Oncogene* 27, 3754–3760 (2008).

14. Tollervey, D. & Kiss, T. Function and synthesis of small nucleolar RNAs. *Curr. Opin. Cell Biol.* 9, 337–342 (1997).
15. Ridanpaa, M. *et al.* Mutations in the RNA component of RNase MRP cause a pleiotropic human disease, cartilage-hair hypoplasia. *Cell* 104, 195–203 (2001).
16. Moriarty, T. J., Huard, S., Dupuis, S. & Autexier, C. Functional multimerization of human telomerase requires an RNA interaction domain in the N terminus of the catalytic subunit. *Mol. Cell. Biol.* 22, 1253–1265 (2002).
17. Lue, N. F. *et al.* Telomerase can act as a template- and RNA-independent terminal transferase. *Proc. Natl Acad. Sci. USA* 102, 9778–9783 (2005).
18. Nakamura, T. M. *et al.* Telomerase catalytic subunit homologs from fission yeast and human. *Science* 277, 955–959 (1997).
19. Mourrain, P. *et al. Arabidopsis SGS2* and *SGS3* genes are required for posttranscriptional gene silencing and natural virus resistance. *Cell* 101, 533–542 (2000).
20. Smardon, A. *et al.* EGO-1 is related to RNA-directed RNA polymerase and functions in germ-line development and RNA interference in *C. elegans*. *Curr. Biol.* 10, 169–178 (2000).
21. Lipardi, C., Wei, Q. & Paterson, B. M. RNAi as random degradative PCR: siRNA primers convert mRNA into dsRNAs that are degraded to generate new siRNAs. *Cell* 107, 297–307 (2001).
22. Sijen, T. *et al.* On the role of RNA amplification in dsRNA-triggered gene silencing. *Cell* 107, 465–476 (2001).
23. Makeyev, E. V. & Bamford, D. H. Cellular RNA-dependent RNA polymerase involved in posttranscriptional gene silencing has two distinct activity modes. *Mol. Cell* 10, 1417–1427 (2002).
24. Semler, B. L. & Wimmer, E. *Molecular Biology of Picornaviruses* 255–267 (American Society for Microbiology, 2002).
25. Behrens, S. E., Tomei, L. & De Francesco, R. Identification and properties of the RNA-dependent RNA polymerase of hepatitis C virus. *EMBO J.* 15, 12–22 (1996).
26. Sugiyama, T., Cam, H., Verdel, A., Moazed, D. & Grewal, S. I. RNA-dependent RNA polymerase is an essential component of a self-enforcing loop coupling heterochromatin assembly to siRNA production. *Proc. Natl Acad. Sci. USA* 102, 152–157 (2005).
27. Masutomi, K. *et al.* Telomerase maintains telomere structure in normal human cells. *Cell* 114, 241–253 (2003).
28. Ford, L. P. *et al.* Telomerase can inhibit the recombination-based pathway of telomere maintenance in human cells. *J. Biol. Chem.* 276, 32198–32203 (2001).
29. Pascale, E., Cimino Reale, G. & D'Ambrosio, E. Tumor cells fail to *trans*-induce telomerase in human umbilical vein endothelial cell cultures. *Cancer Res.* 64, 7702–7705 (2004).
30. Won, J., Chang, S., Oh, S. & Kim, T. K. Small-molecule-based identification of dynamic assembly of E2F-pocket protein-histone deacetylase complex for telomerase regulation in human cells. *Proc. Natl Acad. Sci. USA* 101, 11328–11333 (2004).
31. Almeida, R. & Allshire, R. C. RNA silencing and genome regulation. *Trends Cell Biol.* 15, 251–258 (2005).
32. Schwarz, D. S., Hutvagner, G., Haley, B. & Zamore, P. D. Evidence that siRNAs function as guides, not primers, in the *Drosophila* and human RNAi pathways. *Mol. Cell* 10, 537–548 (2002).
33. Schwarz, D. S., Tomari, Y. & Zamore, P. D. The RNA-induced silencing complex is a Mg^{2+}-dependent endonuclease. *Curr. Biol.* 14, 787–791 (2004).
34. Vagin, V. V. *et al.* A distinct small RNA pathway silences selfish genetic elements in the germline. *Science* 313, 320–324 (2006).
35. Nishikura, K. A short primer on RNAi: RNA-directed RNA polymerase acts as a key catalyst. *Cell* 107, 415–418 (2001).
36. Aoki, K., Moriguchi, H., Yoshioka, T., Okawa, K. & Tabara, H. *In vitro* analyses of the production and activity of secondary small interfering RNAs in *C. elegans*. *EMBO J.* 26, 5007–5019 (2007).
37. Gillis, A. J., Schuller, A. P. & Skordalakes, E. Structure of the *Tribolium castaneum* telomerase catalytic subunit TERT. *Nature* 455, 633–637 (2008).
38. Salgado, P. S. *et al.* The structure of an RNAi polymerase links RNA silencing and transcription. *PLoS Biol.* 4, e434 (2006).
39. Tam, O. H. *et al.* Pseudogene-derived small interfering RNAs regulate gene expression in mouse oocytes. *Nature* 453, 534–538 (2008).
40. Watanabe, T. *et al.* Endogenous siRNAs from naturally formed dsRNAs regulate transcripts in mouse oocytes. *Nature* 453, 539–543 (2008).
41. Babiarz, J. E., Ruby, J. G., Wang, Y., Bartel, D. P. & Blelloch, R. Mouse ES cells express endogenous shRNAs, siRNAs, and other Microprocessor-independent, Dicer-dependent small RNAs. *Genes Dev.* 22, 2773–2785 (2008).
42. Yang, N. & Kazazian, H. H. Jr. L1 retrotransposition is suppressed by endogenously encoded small interfering RNAs in human cultured cells. *Nature Struct. Mol. Biol.* 13, 763–771 (2006).
43. Guggenheim, R., Somech, R., Grunebaum, E., Atkinson, A. & Roifman, C. M. Bone marrow transplantation for cartilage-hair-hypoplasia. *Bone Marrow Transplant* 38, 751–756 (2006).
44. Choi, J. *et al.* TERT promotes epithelial proliferation through transcriptional control of a Myc- and Wnt-related developmental program. *PLoS Genet.* 4, e10 (2008).

Supplementary Information is linked to the online version of the paper at www.nature.com/nature.

Acknowledgements We thank T. Sugimura and S. Hirohashi at the National Cancer Center for comments. We also thank H. Siomi, H. Tabara and Y. Tomari for discussions. This work was supported in part by Grant-in-Aid for Young Scientists (A) 19689010 (K.M.) and Grant-in-Aid for Young Scientists (B) 19791141 (Y.M.) from the Ministry of Education, Culture, Sports, Science and Technology, by the Third-Term Comprehensive Control Research for Cancer (K.M.) from the Ministry of Health, Labor, and Welfare, by a Takeda Science Foundation grant (K.M.), the Uehara Memorial Foundation (K.M.), a J&J Focused Funding Award (W.C.H.) and R01 AG23145 from the National Institutes of Health (W.C.H.).

Author Contributions Y.M., M.Y., M.F., N.O., R.P. and V.K. performed experiments. T.L. and Y.H. designed and carried out the bioinformatics analyses of TERT-associated RNAs. Y.M., M.Y., W.C.H. and K.M. designed the experiments and discussed the interpretation of the results. W.C.H. and K.M. cowrote the manuscript.

Author Information Reprints and permissions information is available at www.nature.com/reprints. Correspondence and requests for materials should be addressed to W.C.H. (william_hahn@dfci.harvard.edu) or K.M. (kmasutom@ncc.go.jp).